Chapter II
Medical Imaging

Conveners: **José Manuel Udias** (Madrid) – **David Brasse** (Strasbourg)

1. Introduction

"A century ago, the living body, like most of the material world, was opaque. Then Wilhelm Roentgen captured an X-ray image of his wife's finger – her wedding ring 'floating' around a white bone – and our range of vision changed for ever". From the words of Bettyann, Holtzmann and Kelves through to the present day, amazing progress has been made in medical imaging. One of the most impressive achievements of the last fifteen years is probably the emergence of molecular imaging.

Multidisciplinary by definition, physicists, biologists, physicians, chemists and mathematicians bring their expertise to observe, characterise and quantify biological processes at the subcellular level in living organisms. Molecular imaging originates from nuclear medicine where single photon emission tomography (SPECT) and positron emission tomography (PET) imaging techniques are used to observe complex biological processes at the early stage of a disease or for therapeutic follow-ups.

The use of radioactive tracers for medical purposes began with Georges de Hevesy in the 1930s. The discovery of technetium at the Berkeley cyclotron and the announcement of the first SPECT machines in 1968 pushed the discipline forward. SPECT rapidly became the most frequently used emission-scanning technology all over the world. The detectors used in SPECT nowadays look quite similar to the ones used at the beginning of this technique. Sodium iodide inorganic crystals, coupled to a matrix of photomultiplier tubes, are well adapted to image the 140 keV photons generated by technetium-99m. The intrinsic performance of most detectors does not impact overall image quality in SPECT, which essentially depends on the collimation stage.

PET began at the same period as SPECT and has overlapped with the other imaging techniques occasionally, but while anatomical imaging modalities such as CT and MR moved under the spotlight of modern clinical practice, PET remained, until very recently, in the shadow. The current success story for PET imaging as an invaluable tool in the clinical routine is due to the combination of several factors,

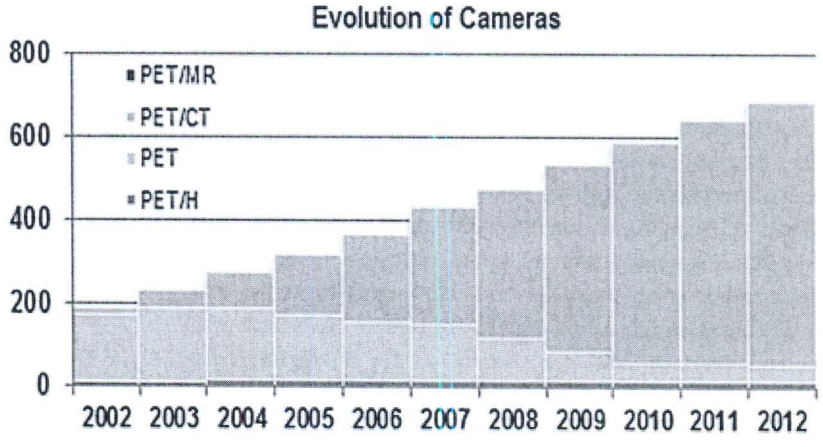

Figure 1. Evolution in the number of PET cameras. It can be seen how PET/CT is now the preferred choice and that the number of PET scanners has sustained a constant growth over the last ten years.

of which improvement in detector performance has in fact played a rather minor role. The need for a "technetium"-like isotope for PET was mandatory. With a half life of almost two hours and ideal physical properties for PET imaging, ^{18}F rapidly became the isotope of choice. However, it requires a well-established network of cyclotron facilities capable of providing radiolabelled compounds at the patient bed. Finding the clinical niche in which PET does not compete with but rather complements other imaging modalities was also a determining factor for the success of PET. The combination with CT promoted PET as the dominant tool in oncology. Johannes Czernin from UCLA, at the 2003 annual DGN meeting, commented that "PET/CT is a technical evolution that has led to a medical revolution".

SPECT and PET imaging techniques are entering a new era, where technical improvements will play an increasingly important role. As an example for SPECT, dedicated cardiac imagers already take full advantage of solid-state detectors. Time-of-flight PET and the combination with MRI will continue to challenge researchers: "PET/MRI is a medical evolution based on a technical revolution", as described by Thomas Beyer.

This chapter highlights state-of-the-art and future prospects of medical imaging, mostly in the field of nuclear imaging. It focuses on new developments and innovations brought by the nuclear physics community. Different sections cover hardware and software developments in clinical and preclinical studies as well as interface applications with other chapters of this booklet.

2. From nuclear to molecular imaging

2.1 Nuclear imaging techniques

Molecular imaging using radioactive tracers makes use of two distinct types of "camera". Tracers containing a radioactive isotope that decays by the emission of a positron are imaged by a positron-emission tomograph. In tomography, a 3-dimensional image of an object is obtained by combining 2-dimensional images taken at different angles around the object. Tracers emitting gamma rays are imaged by the so-called gamma camera. It is used to take 2-dimensional images and, when positioned on a rotating gantry, allows tomographic imaging (SPECT: single photon emission computed tomography).

2.1.1 Positron emission tomography

A typical state-of-the-art commercial clinical PET scanner contains a few tens of thousands of small scintillation crystals that individually detect the positron annihilation photons emitted by the radiotracers in a patient's body. The detection times are measured very accurately, with a precision of about half a billionth of a second. Data rates are large: typically of the order of a million events per second. Sophisticated algorithms distil 3D images out of the huge data set thus recorded. Images with a spatial resolution of about 4 mm are obtained. A whole body scan with the ^{18}FDG tracer, one of the most common PET procedures, takes about 15 minutes.

The scanner bore of about 70 cm is determined by patient size, the axial length of 20–25 cm is a matter of limiting the costs. Nowadays, all PET scanners are combined with a CT scanner for a quick, easy and accurate determination of the attenuation correction needed for quantitative imaging. Scanners come with a collection of sophisticated data and image analysis options for specific scan procedures and clinical investigations. Ease of use and integration in the clinical workflow are well-developed important features.

2.1.2 PET combined with magnetic resonance imaging

In recent years, commercial systems for clinical use combining a PET and an MRI (magnetic resonance imaging) scanner have become available. First systems allowed the integrated but sequential combination of PET and MRI. The development of silicon-based photosensors, which are insensitive to magnetic fields, have made truly integrated systems possible, first for head scans and most recently for full-body scans. These systems allow simultaneous PET and MRI without quality loss in either imaging modality.

2.1.3 Single photon computed tomography

The physical characteristics of SPECT scanners have not changed much over the past few decades. The originally used scintillation material, NaI, remains adequate for the task, mainly because sensitivity and image resolution are largely determined by the collimator positioned in front of the detector. Collimators are rather simple mechanical devices that were optimised quite a while ago. Nevertheless, SPECT scanner developers have made use of the rapid progress in electronics and computation, improving for example ease of use, stability and reliability.

2.2 Preclinical imaging

During the last decade there has been a growing research interest in the field of "molecular imaging". The necessity of understanding biochemical processes at the molecular level have stimulated

a great advance in technological instrumentation, both in hardware and software, especially for in-vivo studies on small animals, e.g. rats and mice. This field of research is often called "preclinical imaging". Major efforts are devoted towards obtaining higher sensitivity, higher spatial resolution and cheaper and easier to handle instrumentation.

This chapter gives a short overview of the state-of-the-art technologies for the most diffuse molecular imaging techniques, namely, positron emission tomography (PET), single photon emission computed tomography (SPECT), X-ray computed tomography (CT) and MRI (magnetic resonance imaging), as applied to small animals. Finally, multimodality techniques that allow the merging of molecular information with anatomical details, such as PET/CT; SPECT/CT and PET/MR, will be illustrated. These are fields where the technology is rapidly evolving.

2.2.1 Present technology for small animal PET imaging

Functional molecular imaging investigations are performed on small animals, such as mice and rats, down to the cellular level, so as to obtain results on simplified human models before direct study on patients [Massoud and Ghambir, 2009]. The requirements on spatial resolution are much higher than those for clinical scanners, because the dimensions of rats and even more of mice are clearly much smaller than those of human beings. For example, imaging of the rat brain requires a spatial resolution of less than 2 mm full width at half maximum (FWHM). A resolution better than 1 mm (FWHM) would be necessary for the brain of the mouse, whereas a state of the art clinical scanner has a spatial resolution not better than 4 mm (FWHM).

In addition, the available radioactive signal is very weak. In fact, the injected activity in a mouse for brain receptor investigation is typically not greater than 5–10 MBq. Further there are limitations on the maximum volume of injected solution (~10% of the total blood volume). As a consequence high-sensitivity instrumentation is especially required when fast dynamic processes are studied with characteristic times of the same order of the scanning time. All of the above has put stringent requirements on PET scanners for small animals and it has produced copious research in this field.

The design of most small-animal PET instruments is usually based on a miniaturised structure of a clinical scanner with small detector elements surrounding the animal in a small bore ring. Other designs make use of rotating planar detector pairs (see Figure 2). The latter configuration offers a better sampling and image uniformity, but it has severe limitations in terms of dynamic imaging and if very fast throughput is desired.

High-resolution multi-anode photomultipliers tubes (MA-PMT) have been the photodetector of choice for most preclinical scanners. In most solutions the MA-PMTs are coupled to pixilated matrices of scintillators. In this case, the coordinates of the photon interaction are obtained via the "light-sharing" technique, i.e. by calculating the centroid of the light produced by the crystal on the high-granularity position-sensitive PMT. MA-PMTs have undergone a series of improvements (see Figure 3) over the last twenty years, many of which have been partly triggered by the needs of the molecular imaging community: this led to the evolution from early MA-PMTs based on a typical round shape, (up to 10 cm diameter, and a crossed wire anode structure), to second generation (square-shaped metal-channel dynode structure) with a very fine anode granularity. And finally, with the third generation there has been a great improvement in the active area dimensions (up to 5 cm inside) and especially in the active-to-total area ratio (up to about 90%). These 5 cm tubes are based on the metal-channel dynode structure with an anode matrix of 16×16 elements on a 3 mm pitch.

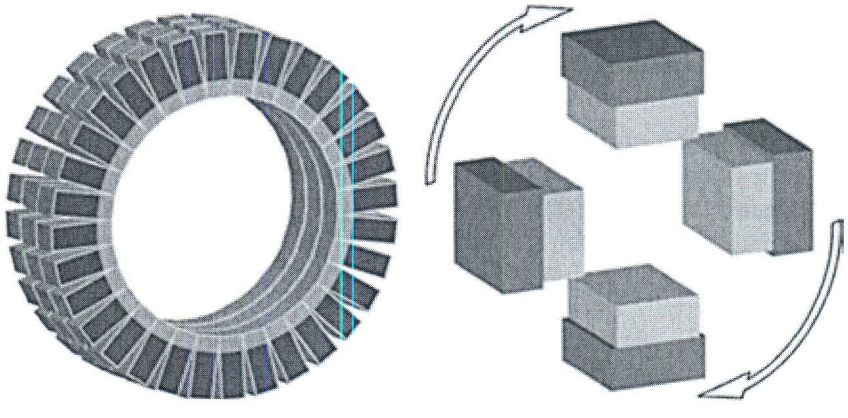

Figure 2. Two different configurations for the construction of a small-animal PET scanner. Left: ring geometry, where the detectors are arranged in rings surrounding the animal. Right: Example of a rotating detectors configuration with four heads, where each one is in time coincidence with the opposite one.

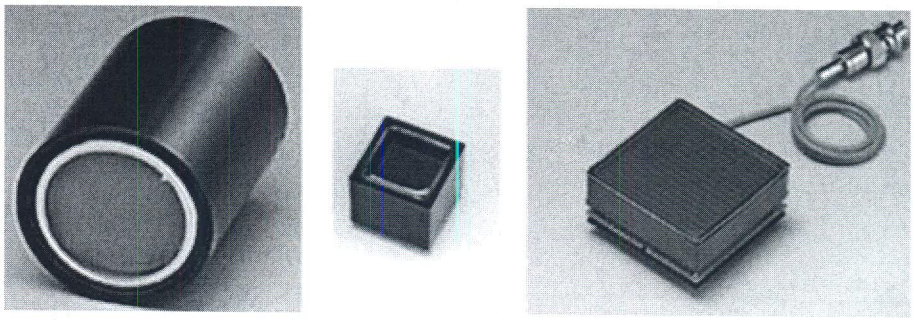

Figure 3. Example of first generation (left, Hamamatsu R2486 with crossed-wire anode structure), second generation (centre, Hamamatsu R8520 with crossed-plate anode structure), and third generation (right, Hamamatsu H8500 with multi-anode structure) MA-PMTs. Images from the Hamamatsu web site: www.hamamatsu.com.

The best readout method for modern MA-PMTs would be independent single anode read-out. To this end, dedicated ASICs have been implemented and are currently used with the H8500 Hamamatsu product in high energy physics. However, in order to limit the cost and complexity of the readout, often the simpler method of resistive chain for both X- and Y-coordinate is adopted, so as to strongly reduce the number of output channels.

More recently, semiconductor photodetectors have become an alternative and more attractive method for the readout of matrices of scintillators. In this case a matrix (either assembled or monolithic) of photoconductors with the same granularity as the scintillator matrix is coupled one to one to the scintillator pixel (no-coding error). Typical examples of this solution are PET inserts to MR, where matrices of small-area avalanche photodiodes (APDs) are used for the parallel readout of the pixilated matrices of a scintillator.

So-called silicon photomultipliers (SiPM) are being characterised and studied by many groups. These photodetectors will definitely not only be used for clinical scanners, but they will replace the so-called block detector. These photodetectors could also be used to reconstruct the centre of mass of the light deposited in a monolithic scintillator, by measuring, with high precision, the centroid of the light spot and also the dimension of the spot, so as to infer depth of interaction (DOI) information.

To maximise the efficiency of PET systems, PET heads should be positioned close to the object, and the thickness of the photon absorber should be at least one attenuation length at 511 keV. With the detector so close to the target, there is a significant contribution of the parallax error to the spatial resolution, and thus many techniques have been developed to obtain DOI information.

The simultaneous improvement of spatial resolution and sensitivity is the challenge of PET imaging. However, these two figures are often mutually opposed, i.e. increasing one could cause the reduction of the other. Every year, new small-animal PET prototypes are produced or proposed by research groups offering or promising even better performance. At the same time, some fully engineered scanners are released as commercial products.

2.2.2 Present technology for small-animal SPECT systems

SPECT systems for small animal imaging are of two main types: the first one makes use of the clinical SPECT configuration, e.g. thallium-doped sodium iodide (NaI:Tl) Anger camera, equipped with a special collimator; the second one consists of dedicated systems based on compact, high resolution detectors, following PET scanner technology.

In both cases, the main feature is the collimator type: contrary to the clinics, where regular arrays of round, square, or hexagonal holes in a high-density medium such as lead or tungsten are used, here the most widely applied collimator solution is the pinhole (or multi-pinhole). With this collimator, one increases the spatial resolution of the imaging system by magnification of the object onto the detector. By using large detectors such as a conventional Anger camera, a very high resolution down to a fraction of a mm is obtained. However, the sensitivity could be very low because of the pinhole configuration. To overcome this problem, multi-pinhole solutions are implemented, but the large magnification produces large projections that may overlap as the number of pinholes increases. The group of Steve Meikle in 2002 has solved the problem of overlapping projections by the use of iterative estimation, originally derived from the coded aperture approach proposed by Harry Barrett in 2001.

As for the second type of small animal SPECT, solid-state detectors provide a promising alternative technology as compact high-resolution gamma cameras. Semiconductor detector technology is the new horizon in dedicated instruments for high-resolution nuclear imaging and such solid-state detectors with direct γ-ray conversion such as CdTe and CdZnTe have been proposed. The requirements for a good detector for SPECT, i.e. high spatial resolution, high energy resolution, and good efficiency for the detection of medium energy γ rays, are only

partially fulfilled by solutions based on scintillators/photomultipliers as in PET, especially due to the low energy resolution of scintillators and the relatively low (25–35%) quantum efficiency of the photodetector. A direct conversion solid state detector offers a much higher quantum efficiency and energy resolution and its granularity is now well within in the range of the necessary high spatial resolution, whereas its intrinsic efficiency does not create a severe DOI contribution, e.g. the mean free path of a 140.5 keV in CdTe is about 2.4 mm.

The major concern for the development of the next generation of PET systems for small-animal imaging is the improvement of sensitivity, always pushing the spatial resolution close to its intrinsic limit. On the other side, small-animal SPECT has almost reached its resolution limit of fractions of a mm. In this case, the main challenge is to increase the sensitivity and especially the field of view to obtain ultrahigh-resolution systems able to visualise the entire animal in one shot.

2.2.3 Small animal CT imaging

Computed tomography (CT) is one of the most widely used techniques of noninvasive diagnosis, which provides a 3D map of the local X-ray attenuation properties of the scanned patient. Dedicated scanners for small animals have been built in the last decades, with the main goal of obtaining a very high resolution, down to tens of microns, and a large field of view so that a scan of the entire animal can be performed in less than one minute. This is obtained by using X-ray tubes with a very small tungsten anode focal spot (~10 micron) and low to medium X-ray energy (30-50 kVp). A large detector, such as magnified CCDs or a CMOS flat panel with a typical pixel size of 50 micron, is used combined with high geometric magnification. The entire system rotates around the animal as in clinical CT in a cone-geometry configuration. Spiral CTs are also implemented. One critical issue for obtaining the design performance is that misalignments in the detectors are kept under strict control during the construction and the use of the CT. This can be done with various techniques, with and without special phantoms. A typical CT image of a mouse is presented in Figure 4.

CT for small animals can operate in step and shoot mode and in continuous mode. The standard way of reconstructing the image employs the Feldkamp algorithm, but iterative methods are being increasingly applied. The main issue with an animal CT is the high dose that is needed for obtaining the requested resolution, i.e. the quantum noise reduction. Hence dose limitation and increase speed of the examination, for instance for angiography studies, are the main topics of research in this field. CT scans have mainly been used in connection with PET images for providing anatomical information to be combined with functional imaging and for calculating the PET attenuation. However, they have also gained importance as a means of investigation *per se* in the field of molecular imaging.

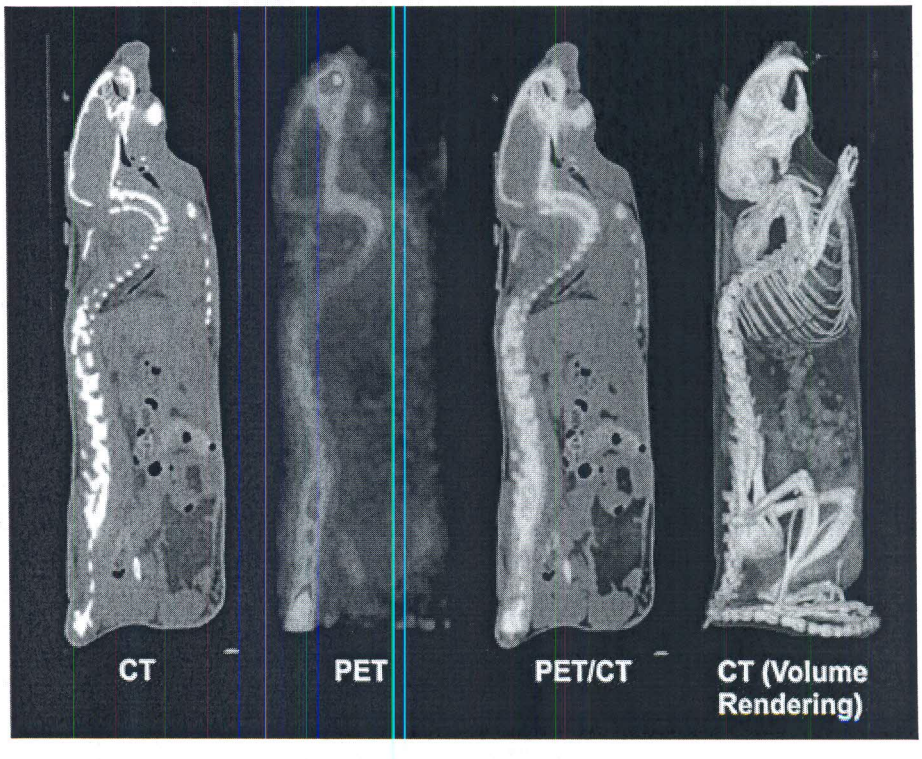

Figure 4. Typical CT image of a mouse: from left to right: CT, PET image (F18-), Fused PET/CT image, CT image volume rendering.

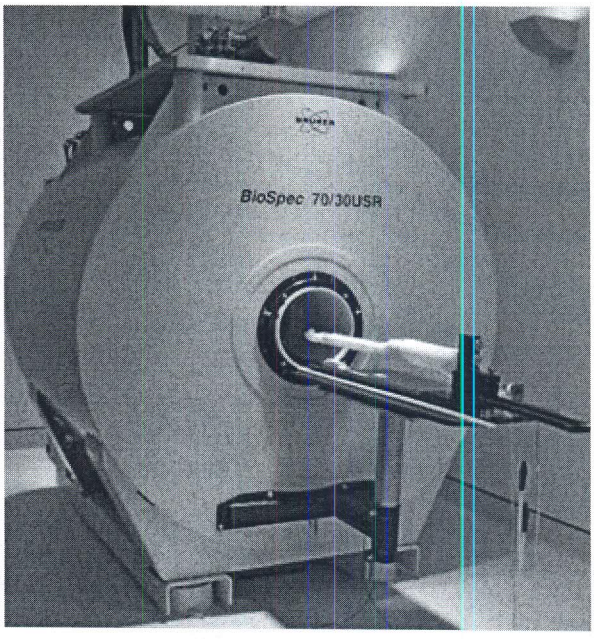

Figure 5. A typical MR system for small animals (Taken from: http://www.weill.cornell.edu/research/cbic/facilities/mri_7tesla.html)

2.2.4 **MRI small animal imaging**

MRI (magnetic resonance imaging) has become a very useful tool both in the clinical and the preclinical fields. MRI can produce images with excellent contrast between soft tissues and with a very high spatial resolution in 3D. Like other imaging techniques, MRI uses electromagnetic radiation to study districts within the subject. Such radiation is non-ionising, so that it can be considered non-harmful for a human subject. However, the interaction of the RF source to produce the MR image can increase the temperature of the body. The quantity that describes this phenomenon is the SAR (specific absorption rate), measured in W/kg and defined as the RF power absorbed per unit of mass of an object. Hence, in-vivo MR imaging requires that the SAR is maintained below a safety limit. To understand the phenomenon of magnetism of the nucleus, one can think of a mechanical analogy with a mass, electrically charged and rotating around its axis. If the centre of gravity of the charge is not on the axis of rotation, the rotation itself generates a small magnetic field in a certain direction. This phenomenon of rotation is called "spin" and causes the nucleus to possess a magnetic moment μ, which aligns along the direction of an external field (B0). An external RF pulse (the so-called B1 field) can transfer energy to the nucleus that will flip its magnetic moment according to the energy received, typically by 90 or 180 degrees. Within a certain relaxation time, the magnetic moment will return to its stable equilibrium position. The measurement of the relaxation times T1 and T2 gives an insight to the distribution (morphology) and behavior of the hydrogen (i.e. of the water) in the body (physiology). The phenomenon of magnetic resonance can be investigated using different types of nuclei (^{1}H, ^{13}C, ^{19}F, ^{23}Na, and ^{31}P) with an appropriate RF operating frequency to match the Larmor frequency of the nucleus under study. For small animal imaging, MRI is a very versatile technique capable of providing a very high spatial resolution (100 micron or less) for rodents. The strength of the magnetic field may vary from 0.5 to 9.4 T according to the application and of course to the cost of the apparatus. An example of a 7 T system from Bruker is shown in Figure 5. The system has a diameter of clear bore >30 cm.

The impact of MRI in molecular imaging is continuously growing: examples are translation studies for angiogenesis and phenotypic characterisation, dynamic visualisation of tissue perfusion, and many more. The step-up from MRI and MRS has been favoured by high field systems, which allow for a higher signal to noise ratio. The identification of different atomic nuclei provides insights to functional and biochemical information: for instance cell membrane studies, creatine and lactate quantitative studies, etc. The limit of MRI and even more so of MRS is its sensitivity, still in the micromolar range, as compared to PET and SPECT. Thus, the MRS studies with ^{1}H, ^{19}F, ^{31}P and ^{13}C MRS compounds in preclinical research are primarily confined to pharmacodynamic, but not pharmacokinetic studies. With the advent of high field (i.e. 9.4 T) and the advanced shimming high-resolution proton spectra, studies of the mouse brain have been receiving great attention, especially for tumour response and fMRI.

2.2.5 **Multimodal approach**

2.2.5.1 **PET/CT and SPECT/CT**

Functional imaging such as PET and SPECT are intrinsically non-morphological techniques. Hence anatomical information is often mandatory to localise precisely the position of the radiotracer. In addition, when quantitative information on small target sites is needed, anatomical images are needed to apply proper corrections for partial volume error. In any case, it is obvious that the information from a morphological imaging technique, such as CT or MR, is of great help for the PET or SPECT image analysis. More and more integrated systems are required in analogy to the clinical area, where a PET/CT is the diagnostic instrument of choice for most investigations. Also in the field of small animal imaging, there are two types of multimodalities, the so-called "tandem configuration", where the two modalities are executed one after the other, sharing the same bed for the animal such as in PET/

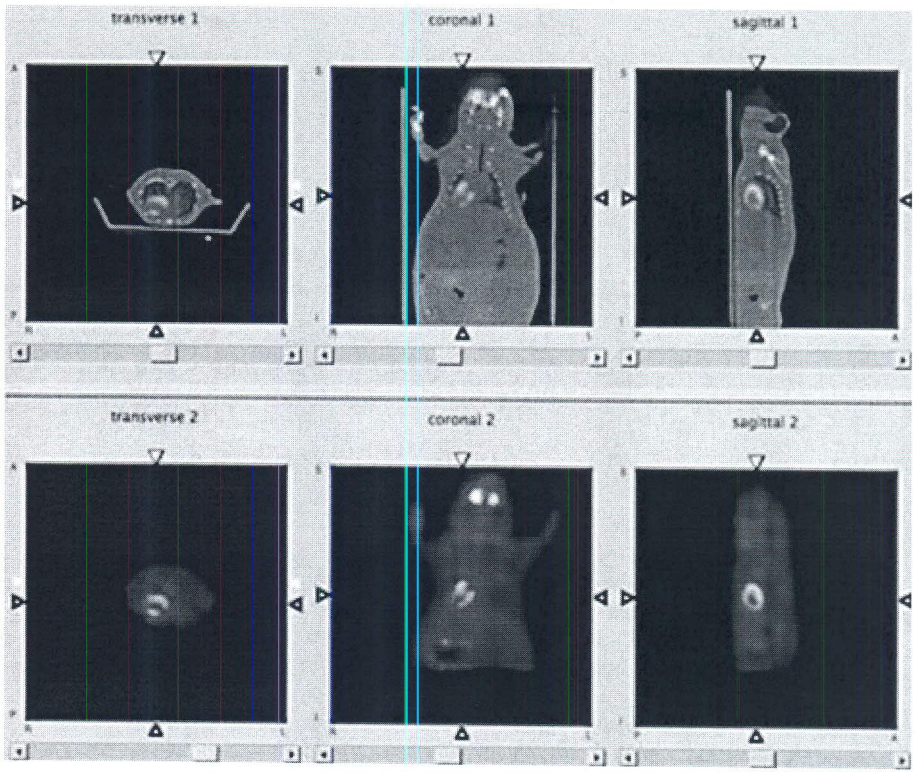

Figure 6. Typical imaging performance on one of the most recent preclinical examples (IRIS, raytest-IVISCAN). Top: PET/CT image obtained with the IRIS PET/CT scanner; bottom: PET image only (courtesy of Panetta D and Salvadori P, IFC-CNR, Pisa, 2013).

CT, SPECT/CT, PET/MR and SPECT/MR, and the truly combined modality, this latter type is only implemented as of today in PET/MR.

In the shadow of the successful application of combined PET/CT scanners in the clinical environment, this technique has been recently transferred to small-animal scanners. In fact, the morphological information from CT can be used to obtain a finer spatial localisation of the radiotracer distribution within the body as well as to obtain the attenuation coefficient map of the object under study for attenuation and scatter correction of the PET images.

CT images are mostly used to improve the emission images. In fact, the emission images are affected by a quantitative error due to the attenuation of radiation by the object under study. Even when this effect is much smaller than for humans, the magnitude of this correction in small animals is non-negligible. For example, in PET the attenuation correction factor is 4.5 for a 40 cm diameter man, and is 1.6 for a 5 cm diameter rat, and 1.3 for a 3 cm diameter mouse. In the CT case, the attenuation coefficients are measured with a continuous X-ray spectrum, ranging from 10 to 70 keV. Hence the CT-energy linear attenuation coefficient (μCT, X) has to be scaled to the 140.5 keV value for SPECT by a linear formula and for PET to 511 keV by a bilinear interpolation. Figure 6 shows typical images obtained without CT (bottom) and with CT corrections and image fusion (top).

2.2.5.2 **PET/MR**

Early diagnosis and therapy are connected to molecular imaging and genetic information. As for molecular imaging, the multimodality approach is becoming increasingly necessary. In fact, the combined systems PET/MR and SPECT/MR have received great attention and development. The advent of new solid state detectors such as APDs, PS-APDs, MPPCs and SiPMs has allowed the insertion of a PET system within the high magnetic field of an MR. It is well known that to have quantitative PET information an attenuation correction must be performed, best made with a CT. This was the reason for introducing PET/CT systems in the clinical, and also in the preclinical, field. As for the MR based attenuation correction, a lot of research has been going on to find the best way to do it: segmentation, brain atlas, and special sequences (i.e. UTE) have been proposed in combined modalities. MRI and PET in the preclinical scenario are now mostly in the same system, either as a PET insert or as a combined structure from the beginning. MRI and PET offer complementary functionality and sensitivity. Simultaneous acquisition capitalises on the strengths of each, providing a hybrid technology that has a significantly greater impact than the sum of its parts. A schematic scheme of the structure of a typical combined system is depicted in Figure 7.

Among the many applications with a combined PET/MR it is worth noting: dynamic studies, MR/PET cross correlation, MR-guided motion cor-

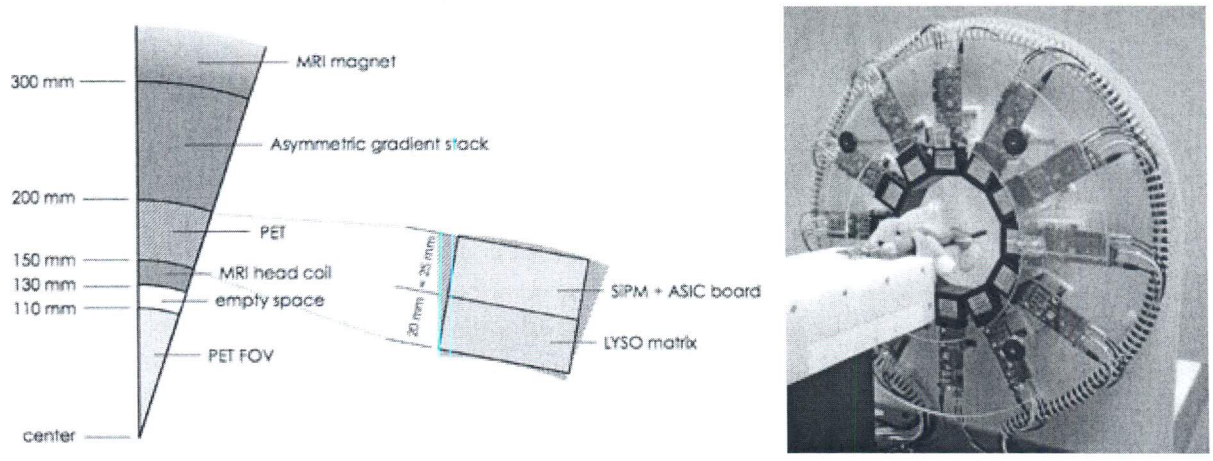

Figure 7. Cross section of the combined PET-MR system proposed for the TRIMAGE PET-MR-EEG project (courtesy of A. Del Guerra, 2013).

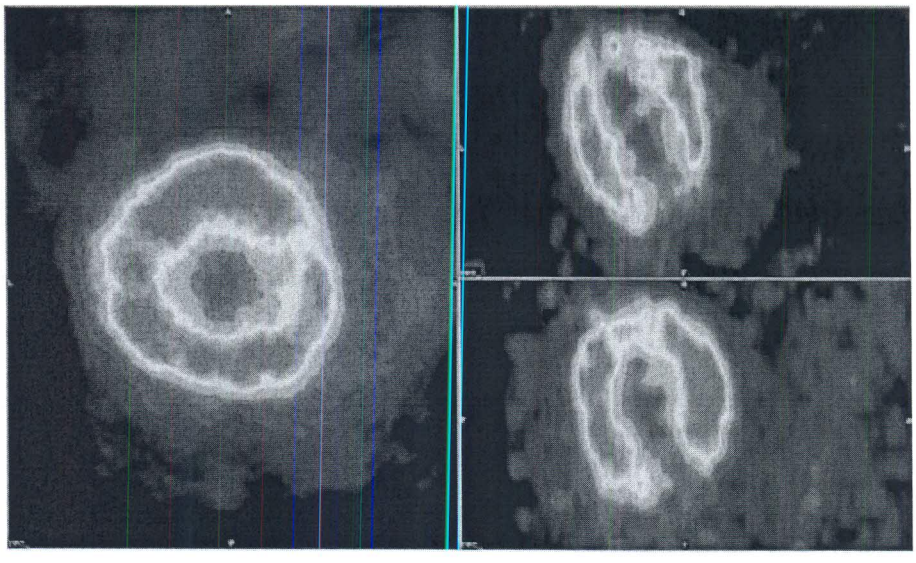

Figure 8. Image of an FDG-injected rat heart obtained in the combined PET-MR MiniPET-3, a SiPM based small animal scanner for molecular imaging developed by MTA Atomki, University of Debrecen (Hungary), ST Microelectronics and Philips Applied Technologies in the frame of ENIAC CSI.

rection of PET and PET image reconstruction. Preclinical PET/MRI scanners based on APDs or magnetically shielded PMTs are on the market. Several detector prototypes based on SiPM are being developed.

3. New challenges

Multi-modality imaging is used to show both the molecular processes taking place in the body and the anatomical location in which they are happening so that, for example, a tumour can be detected using PET imaging and located using CT in a PET/CT scanner. PET/CT was introduced 15 years ago and multi-modality is standard for SPECT and PET machines which are now on sale. Commercially, multi-modality means SPECT/CT or PET/CT.

The new challenge is to combine MR imaging for anatomical location with PET and SPECT. The benefits are to reduce the radiation dose by eliminating the CT scan, and the possibility to use functional MRI as well as simple anatomical MR scans (so that blood flows, for example, can be detected). However, this is technically more difficult because typical SPECT and PET scanners use scintillators with photomultipliers that are incompatible with the intense magnetic fields of modern MR scanners. The rotating gantries used in PET and SPECT can also be affected by the MR magnetic field. Conversely, the PET detectors must not affect the sensitive MR scanner operation either by perturbing the field or introducing electrical noise.

Although PET/MR multi-modal imaging has been in use for a few years it was, until very recently, done sequentially rather than simultaneously. Clearly simultaneous imaging is preferable, for example to avoid motion artefacts between scans, and the first simultaneous PET/MR scanners are now coming on the market (e.g. Philips Biograph mMR). Technology from nuclear physics detector systems is used to overcome the magnetic incompatibility. Some preclinical prototypes used light guides to allow photomultipliers to be located further from the magnetic field, however the more popular route seems to be to use of semiconductor light sensors (APDs or SiPMs) to replace the photomultipliers or to replace scintillators by semiconductor detectors.

The next challenges yet to be solved in the commercial market are to integrate SPECT with MR and to integrate fast detectors for TOF PET in an MR environment for simultaneous operation (sequential TOF PET/MR exists). MR-compatible TOF modules can be made using nuclear physics detectors (fast scintillators with SiPMs) as building blocks for TOF PET/MR. SPECT/MR is far from market while research systems use semiconductor detectors to replace the scintillators either by putting CZT detectors behind the SPECT collimators or else by electronic collimation using a Compton camera made of semiconductor detectors.

These last two (SPECT/MR and TOF PET/MR) are the challenges, where techniques from nuclear physics systems are currently making a difference and enabling the development of new multimodal imaging systems.

3.1 Detector design

Despite the excellent performance reached by PET detectors, there is room for improvements that will also allow non-standard use of PET technology, such as in-beam measurements during particle therapy sessions.

Research is being carried out worldwide in order to improve all the relevant aspects that contribute to the overall performance of a PET scanner: detection efficiency, spatial resolution, depth of interaction measurement, time resolution, compactness, MR compatibility, speed and power consumption.

All the PET components reviewed in the following, as well as the strategic choices in the design

of the global systems, are subject to continuous research and development, with the ultimate goal of providing the most accurate input information to the 3D or 4D reconstruction algorithm.

3.1.1 Scintillators

To be used as a primary photon converter for a PET (fixed photon energy) and a SPECT (wide photon energy range) detector, a scintillating crystal must meet the following requirements:

- high density (i.e. high conversion efficiency);
- high light yield (related to the energy and time resolution);
- short rise time to optimise the time resolution.

The figure of merit that summarises the suitability of a crystal is usually defined as:

$$\eta \sim \varepsilon^2 \sqrt{N/\tau}$$

with ε, N, τ related to the crystal density, light yield and decay time, respectively.

In addition, the technology must provide uniform crystals at a low (acceptable) cost.

The state of the art for PET/SPECT scanners is a set of inorganic crystals, whose properties are summarised in Table 1. LSO and LYSO are the best choice for scanners that also aim at the time of flight measurement. However, the search for new materials that would better meet the requirements for a more efficient and time performance scanner has not stopped and in recent years some new candidates have emerged.

As an optimal timing resolution is related to the photon counting statistics, it requires the capability to trigger at very low threshold, with the performance limit being reached when counting single photons. When these conditions are met, a high light yield and a short rise-time of the scintillating light allow the best measurement of the interaction time, with the theoretical possibility to approach a limit value of about 100 ps.

GAGG crystals have been recently studied as a possible alternative to known scintillators for PET and SPECT scanners: the density, light yield and time resolution are suitable, but suggest a possible marginal improvement rather than a significant step forward.

Plastic scintillators, which would provide a very short decay time, suffer from low stopping power and insufficient optical photon yield. However, novel methods developed in the last few years allow increasing thickness of the plastic detector and at the same time determination of the depth of the interaction of the registered gamma quantum. In addition, thanks to the large solid angle covered by new PET devices under construction, the decrease of the detector efficiency will be compensated by the increase of the acceptance. The small efficiency for the photoelectric effect in organic scintillators worsens the image quality due to a low ability to distinguish between quanta reaching the detector directly and quanta re-scattered in the body of a patient. This drawback is compensated by the selection of only these events for which the energy deposited in the scintillator corresponds to the range close to the maximum of energy which can be transferred to the electron via the Compton scattering process, and by taking advantage of the excellent timing response of organic scintillators, allowing for the effective usage of the TOF technique.

Should the scintillators be engineered with a photonic crystal pattern, the light collection at the surface would be improved. However, despite some promising preliminary results, the technology is still in an early stage.

Table 1. Properties of the most used scintillator in PET and SPECT [Adapted from Lecomte R. *Eur J Nucl Med Mol Imaging* **36**, n° Suppl. 1 (2009): S69–S85.]

	NaI	BGO	GSO	LSO	LYSO	LGSO	LuAP	YAP	$LaBr_3$
Light yield 10^3 ph/MeV	38	9	8	30	32	16	12	17	60
Primary decay time	250	300	60	40	41	65	18	30	16
ΔE/E (%) at 662 keV	6	10	8	10	10	9	15	4.4	3
Density (g/cm³)	3.67	7.13	6.71	7.35	7.19	6.5	8.34	5.5	5.08
Effective Z_{eff}	50	73	58	65	64	59	65	33	46
1/μ@511keV (mm)	25.9	11.2	15.0	12.3	12.6	14.3	11.0	21.3	22.3
PE (%)@511 keV	18	44	26	34	33	28	32	4.4	14

PE: photopeak efficiency

3.1.2 **Photon detectors**

Once the primary photon conversion efficiency and the secondary photon light yield and collection rate are optimised, a high performance photon detector is required in order to exploit the raw information at best.

Clinical PET and SPECT scanners are typically based on photomultipliers (PMTs), which, despite the high gain, do not meet two important requirements: compactness and magnetic field compatibility.

In recent years, research projects have focused on directly providing digital output.

APDs, that are insensitive to magnetic fields, were used for the first commercial PET/MR scanner; however, their drawbacks (low gain and long rise time) make them unsuitable for high performance TOF-PET.

SiPMs, on the other hand, besides meeting the requirements of compactness and magnetic field insensitivity, present a very interesting advantages: low bias voltage makes them even more attractive than APDs for hybrid PET/MR imaging, while high gain and short rise time make them the best candidates for TOF-PET. The short rise-time and the high level of homogeneity of SiPM matrix components should be compatible with a time resolution that could approach the lower limit of 100 ps. In addition, the high gain could allow single photon counting, which, if the dark count rate is kept under control with active cooling, would make it possible to design a detector that couples continuous crystals to segmented SiPM matrices.

dSiPMs, developed by Philips, are based on the integration within the SiPM sensitive area of basic processing electronics and eliminate the need for external processing. Each micro-cell of the array is connected to an integrated counter and an integrated TDC that provide the energy and time information, respectively. dSiPM coupled to LYSO crystals reach time resolutions as low as 150 ps (FWHM). The various performances of these devices are summarised in Table 2.

Ultra Fast Silicon Detectors (UFSD) are a new promising technology for the improvement of spatial resolution, while keeping a time resolution of the order of 100 ps. Their possible performance limit, however, is in their low gain (5–15), which could deteriorate both the signal to noise ratio and the related time resolution with respect to the nominal expected values. The construction and characterisation of the first prototypes will require special attention to the capability of detecting the first secondary photons emitted in the crystal de-excitation process, which are key to an excellent time resolution. Should this limitation be overcome, UFSD would be an excellent candidate for hybrid PET systems, thanks to their compactness and intrinsic insensitivity to temperature and magnetic fields.

Semiconductor detectors based on CdTe or CdZnTe are solid-state devices that allow the direct conversion of gamma rays to electrical charges. The conversion yield is large with respect to scintillation devices: typically 30000 charges for a 140 keV energy release. As a consequence, the energy resolution is not limited by charge generation statistics but by other phenomena, such as electrical noise or material uniformity. While the best devices achieve better than 2% resolution at 140 keV thanks to an optimised design, typical resolution values by standard systems are close to 5% at 140 keV, a value that can help the development of dual-isotope imaging protocols.

The spatial resolution of these semiconductor detectors can be extremely good, as it is not limited by light spreading and photon statistics, but rather by the readout circuitry. A typical device resolution is of the order of 2.5 mm, but the use of high density readout or sub-pixel positioning electronics allow for an intrinsic resolution of few hundreds of micrometers (200–400μm).

CdTe- or CdZnTe-based detectors are integrated in small modules that couple the semiconductor crystals and the readout electronics on the same

Table 2. The most important parameters of (secondary) photon detectors.

Detector	PMT	APD	(d)SiPM	UFSD
Gain	10^5	50-1000	~ 10^6	5-15
Rise Time (ns)	~ 1	~ 5	~ 1	~ 0.1
Quantum Efficiency (QE) @ 420 nm (%)	~ 25	~ 70	~ 25-75 (PDE)	~ 75
Bias (V)	> 1000	300-1000	30-80	100
Temperature sensitivity (%/K)	< 1	~ 3	1-8	Negligible
Magnetic field sensitivity	Yes	No	No	No

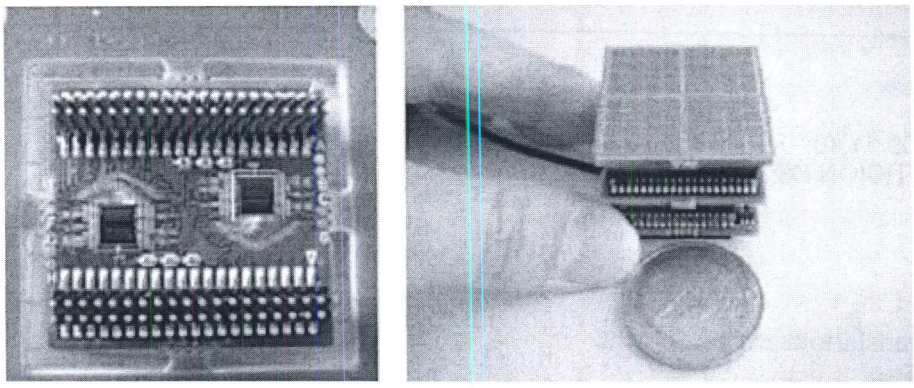

Figure 9. Example of compact front-end electronics to read-out a SiPM matrix.

substrate. System designers have profited from the compactness of such modules to build innovative SPECT tomographs that exploit the modularity to enhance sensitivity and resolution by focusing of a given region of interest. Additionally, these systems also avoid the motion of the camera head around the patient.

3.1.3 **Front-end electronics**

Front-end electronics is becoming a key enabling technology (KET) for detectors due to the increasing number of channels and the high level of integration that allows reductions in cost and dimensions. A general trend is to integrate more and more functions in ASICs (amplification, filtering, digitisation, signal processing), making them systems on a chip (SoC). These multi-channel ASICs also tend to move closer or even onto the detectors, minimising the connections and improving both performance and reliability. This localisation coupled to the increasing number of channels requires low-power designs, so that the performance and compactness obtained are not spoiled by large cooling systems. The evolution of microelectronics technologies allows this increase of performance together with power reduction and higher operating speeds, an important feature for reducing a patient's exposure, while maintaining high quality resolution.

Such a design is also useful from the point of view of the system performance, since it allows more accurate timing measurements that improve the noise and background reduction and therefore provide better quality images with lower doses delivered to patients.

3.1.4 **Module layout**

State-of-the-art scanners are based on segmented crystals that collect most of the secondary photons on a single channel, which are then detected by PMTs, APDs or SiPMs, whose signals are processed by dedicated ASICs and FPGAs.

Any change in the detector design is related to possible improvements of the key parameters that describe the overall system performance: efficiency, 3D spatial resolution, time resolution, MR compatibility, compactness, speed and power consumption.

The scintillator, selected according to the figure of merit already discussed, is usually segmented and placed radially with respect to the annihilation volume.

Recently, two alternative designs have been proposed. The segmented crystal could be placed axially, with several long (up to 10 cm) and thin layers: such a design provides an excellent DOI measurement, while the axial position along the crystal is obtained via the light sharing and/or the time difference read on the opposite sides.

The availability of high performance segmented SiPM matrices, with high gain and the possibility to detect single photons, prompted some projects based on continuous scintillator blocks read by segmented matrices. The continuous crystal would allow a cluster reconstruction, with the double advantage of using the cluster size for the DOI measurement and of a multi-sampling of the secondary photon time distribution, which would help improve the TOF measurement. Such an approach strictly depends on the capability to control the SiPM dark count rate, so as to limit the trigger rate and to distinguish contributions to the cluster reconstruction from channels triggered by dark counts. This result can only be achieved with a cooling system that allows a temperature stability within about 1°C.

SiPMs (analogue or digital) are the photon detector of choice for almost every ongoing research project: they are efficient, with very high gain, single photon counting capabilities, very high spatial resolution and excellent timing resolution (with intrinsic resolution among the different cell contributions to a matrix element quite close to 100 ps). They are also compact, compatible with operations in a magnetic field and acceptably priced.

Custom front-end electronics developments mostly focus on optimising the TOF measurement, so as to reach an overall resolution in the 100–150 ps range. If the scintillator rise-time and the pho-

ton detector signal formation time are short enough and the detector uniformity in the time response is good (as it is for the latest SiPM matrices available on the market), the front-end electronics contribution can become the main source that contributes to the system time resolution. Whether the crystal is segmented or continuous, the key to optimise the time resolution is the capability to identify the first photon(s) from the crystal de-excitation and to distinguish them from the spurious dark count signals. With a segmented crystal, the analysis of the rising signal shape is the clue, while in the case of a continuous crystal, where the threshold must be as low as required to detect single photons, the cluster analysis algorithm must be able to distinguish true signals from dark count background events.

An important innovation to real-time data handling could come from the concept of "deferred coincidence". Single events can be routed to a ring network, which provides real-time processing and coincidence determination within the network itself; this simplifies the construction of the overall system and allows its scaling to larger detector arrays.

The need for precise temperature control and uniformity is also being addressed by designing active cooling systems that are very important to keep the system performance constant.

System compactness and MR design compatibility are also provided by the choice of solid-state photon detectors such as SiPMs.

System compactness is particularly important when developing a detector for an endoscopic approach, which, combined with timing resolution, will allow more sensitive, more precise, lower radiation doses and less invasive imaging and intervention on small internal structures and lesions.

Ultimately, all of these features point towards earlier detection and patient-tailored treatment of asymptomatic cancer types.

3.1.5 **New detector concepts**

Several new approaches to the detection of primary photons originating in the e^+e^- annihilations have been proposed, and are described below.

Resistive plate chambers (RPC) are gaseous parallel plate detectors for charged particles widely used in large-scale high energy physics experiments, and could in principle replace the crystal scintillators, as well as the secondary photon detectors in a PET system.

RPCs provide excellent time (20–30 ps) and spatial resolution (hundreds of microns), work well in strong magnetic fields and are inexpensive, so that large area detectors (~2–3 square metres) can be built, providing a large field of view and increasing the geometrical acceptance with respect to standard PET devices.

The low detection efficiency for 511 keV photons (<30%) is a major drawback, as it implies a much larger number of annihilations to provide statistics comparable to standard PET systems and therefore the dose delivered to the patient will increase.

Still, investigation of RPC-based PET as a candidate for PET/MRI hybrid imaging and in-beam PET measurement is ongoing.

Liquid calorimeters are also being considered as an alternative to standard PET systems. TriMethyl bismuth (TMBi) is an innovative liquid that efficiently converts photons of energy less than 1 MeV through the photoelectric effect. The light produced by a relativistic electron is detected in a time-projection ionisation chamber, supplemented by a photo-detector. The simultaneous detection of light and charge signals leads to a very promising performance in positron-annihilation detection. A spatial resolution of 1 mm^3, a sub-nanosecond timing, and a photon energy resolution of about 10% FWHM are foreseen, with a single interaction (photoelectric) conversion probability above 47%, a value still unsatisfactory when addressing the dose minimisation issue.

To improve the time resolution, the exploitation of the Cherenkov effect, which bypasses the scintillation process and provides almost instantaneous response to incident 511 keV annihilation photons, is being investigated. Cherenkov photons were shown to have significant influence on the rise time of inorganic scintillators – a key-feature for the time measurement and extensive research on this topic might lead to improved time resolution of PET detectors. According to simulations performed by Brunner et al., the intrinsic time resolution could be as low as 30 ps, if appropriate front-end electronics were available.

3.2 **Simulation and reconstruction**

Contrary to planar imaging, which includes scintigraphy, or radiography, tomographic images are not directly obtained from the measurements, but are the result of the so-called *tomographic* or *image reconstruction* process. Classically, the goal of tomographic reconstruction is to obtain the image of an "object" from its "projections", where the object might be an attenuating medium (CT) or a radioisotope distribution (PET, SPECT or Compton cameras). Tomographic image reconstruction is a process based on mathematical algorithms that

are implemented in computers. Although a mathematical solution for the problem of tomographic reconstruction was first proposed in 1917, the advent of modern computers made CT a reality. Computers are also essential to simulate the complex physical phenomena that underlie the image formation process, such as the behaviour of optical photons within scintillation materials, the radioisotope decay and subsequent radiation emission, etc. Continuously increasing computing power has enabled the development of more sophisticated image reconstruction algorithms, and more detailed and accurate simulations of tomographic systems. In this section, we will present state-of-the-art research and the most recent advances in image reconstruction and simulations.

3.2.1 Image reconstruction

Traditionally, a tomographic image corresponds to a plane section (2D image) of the object under inspection. A volume (3D image) is thus constructed by aligning several reconstructed sections. Nowadays, modern reconstruction techniques can directly provide 3D images (fully 3D reconstruction) and 4D images if time is also taken into account; 4D image reconstruction is particularly useful in cardiac PET and SPECT, or to image regions affected by respiratory motion, and it is essential in dynamic emission tomography, whose goal is to study the concentration of the injected tracer over time.

At present, there are several image reconstruction algorithms, which can broadly be divided into two categories: analytic and iterative reconstruction methods. Analytic reconstruction methods are based on a direct mathematical solution, and are still widely used for CT reconstruction. However, the assumptions on which analytical methods are based usually do not hold in emission tomography.

Compared to analytical reconstruction, the main advantage of iterative methods is their ability to include a more accurate description of the imaging process, which in turn, usually leads to better images. This is particularly the case when the measurements are noisy, or when the imaging device cannot provide uniform or complete sampling (see Figure 8). Therefore, iterative reconstruction methods are preferred in emission tomography, although analytical methods, such as filtered backprojection (FBP) are still used for quantitative image analysis in spite of their limitations.

The goal of iterative reconstruction techniques is to find an image estimate by successive steps. In the last few decades, a wide variety of algorithms have been presented. We refer the interested reader to some excellent reviews (such as that by Defrise & Gullberg 2006).

Most iterative reconstruction techniques share the same 'ingredients': models for the image, the data and the imaging system, an objective function, and an optimisation algorithm. The underlying physics of the image formation and degradation phenomena can be taken into account in the choice and description of the models, as well as in the design of the cost function, as will be described in the following paragraphs.

3.2.1.1 Physics and iterative image reconstruction in emission tomograhy

One of the main strengths of iterative algorithms lies in their ability to include accurate models of the underlying physics, which include the statistical nature of radioactive decay or radiation detection, and the interaction of radiation in matter. The statistical nature is contemplated within the data model. Most commonly used reconstruction techniques are based on a Poisson model; this model naturally leads to the Maximum-Likelihood (ML) criterion to determine which image is the best estimate of the true object.

The behaviour of the imaging device is described within the so-called system response model or system response matrix (SRM). In PET or SPECT, the elements of the SRM correspond to the detection probability of gamma rays originating from a certain location. In the first place, the effects of the geometry and arrangement of the detector elements on the detection (and the collimator in SPECT) should be modeled. The system model can also include a description of crystal penetration effects, cross-talk, inter-crystal scatter, etc. In principle, the more effects that are correctly modeled and included within the SRM, the better the reconstructed image. However, computing the SRM for a certain device can be very challenging given the dimensions of the matrix, which corresponds to NxM, N and M being the number of data and image elements, respectively. For a conventional clinical PET scanner, N can be larger than 10^8, and the image might be composed of several millions of voxels. The more physical effects that are contemplated, the less sparse the SRM becomes. Several techniques have been proposed to compute and handle the SRM. Factorisation of the SRM in several components makes it easier to calculate and store the SRM, and to handle it during the reconstruction. Monte-Carlo simulations have proved to be a very useful tool to compute the whole SRM or several of its components for PET and SPECT. Approaches based on measurements can provide very realistic models for the Point Spread Function. Analytical models usually allow for faster but less accurate

alternatives; analytical comprehensive models have been also proposed, but the computational cost can be prohibitive. In any case, since the factorisation of the system matrix allows the contribution of the various physical phenomena to be calculated separately, different approaches can be combined to calculate the various components of the system response model. Finding a balance between computation cost and model accuracy is currently a very active field of research.

Patient-dependent effects, such as attenuation or scatter, can be also included within the reconstruction process. Attenuation factors, previously obtained from CT, MRI or additional measurements, are built within the SRM. Some attempts have been made to include object scatter within the SRM, for example using Monte-Carlo simulations; however, the most common approach is to use the scatter estimate within the comparison step of the iterative algorithm. In this step, the measured data are compared to the ideal data that would have been measured for an object being described by the last image estimate. For PET, the contribution of accidental coincidences can also be taken into account in the comparison step.

As mentioned above, the increasing number of detection channels and the subsequent need of smaller image elements poses several challenges in the computation and handling of the SRM. Much effort has been expended in the last few years to optimise the balance between accurate models and computational efficiency. A way to avoid the storage of the SRM is to calculate the system model on-the-fly. This approach is usually the one chosen when dealing with "list-mode data", i.e. the measured data are not compressed into histograms (such as sinograms), but are stored accorded to the registration time. List-mode reconstruction makes it possible that the whole information contained in the data is preserved and exploited. This is done usually at the cost of simplified system models, since the latter are calculated on the fly; however, fast but accurate system models for list-mode reconstruction, usually based on analytical approaches, have been proposed lately.

Time information is the key in time-of-flight (TOF) PET, which requires dedicated algorithms to exploit the location constraint for the positron-electron annihilation provided by the time difference in the arrival of the two annihilation photons. This technology, proposed in the 1980s, has been recently translated into clinical PET. In combination with dedicated algorithms, TOF PET allows image quality (in terms of SNR and lesion detectability) to be improved.

Concerning the image model, rectangular voxels are the preferred option. In the last few years, spherical based functions ("blobs") have deserved renewed attention given their ability to reduce image noise, but usually at the expense of higher computational cost. Other potentially interesting alternatives are polar pixels, which allow the symmetries of the imaging device to be exploited, or those based on irregular grids.

The cost function and its optimisation are the 'core' of a reconstruction algorithm. Most widely used techniques are based on the optimisation of the aforementioned ML criterion, the Maximum-Likelihood-Expectation-Maximisation algorithm (MLEM) and its accelerated version Ordered-Subsets-Expectation-Maximisation algorithm (OSEM) being the most popular ones. However, the ML estimation problem is ill-conditioned, which results in unavoidable noise in the data causing noisy images. Noise regularisation is thus needed, which can be achieved through early stopping (before convergence), post-reconstruction smoothing, or by adding a penalty function in the objective function. The latter approach can also be derived if the problem is formulated in a Bayesian framework (Maximum-a-Priori algorithm, MAP). The penalty function (or prior) might also include some anatomical information of the patient obtained from a CT or MRI. Compressed sensing (CS) reconstruction approaches and CS-based total variation (TV) regularisation are earning much interest in the community, especially for CT. TV priors offer a promising alternative to compensate for missing data, such as those arising from gaps between detectors or partial PET ring configurations.

3.2.1.2 Accelerating iterative image reconstruction

One of the main drawbacks of iterative image reconstruction is its computational cost. Not only might the calculation of the system response matrix be computer expensive, but also the image reconstruction process as such. Therefore, much effort has been devoted to accelerate the reconstruction process, which remains an active field of research. Some of the proposed approaches rely on parallel computing using clusters, or multicore architectures; the use of graphical processor units (GPUs) has earned much attention in recent years as a cost-effective alternative, especially useful for TOF PET. A completely different approach is to implement the reconstruction within a field programmable gate array (FPGA).

3.2.1.3 Image quality, quantification and compensation of degradation phenomena in ET

Tomographic images can be employed for different purposes. PET and SPECT are commonly used for diagnostics and therapy follow-up in clinical routine. More recently, PET images are also used for tumour delineation in radiotherapy planning. At the same time, emission tomography of rodents and larger animals (such as monkeys for neurosciences and pigs for cardiology) is a common tool in biomedical research, or pharmacology. It is obvious that, for any of these applications, the quality of the image should be "as good as possible". On the other hand, the kind of information to be extracted from a reconstructed image depends on the final purpose: visual inspection, lesion detection, quantification of certain physiological parameters, etc. In the end, this purpose will determine which are the main properties or characteristics that a "good image" should exhibit and which, in turn, the reconstruction algorithms of choice should be able to provide.

Quantitative image analysis (quantification) consists of extracting certain parameters of interest from an image, for example tracer uptake. To obtain quantitative information, a linear relationship is required between image voxel values and activity concentration. For this purpose, several effects need to be accounted for; some of these effects are related to the underlying physics and image formation processes and are thus unavoidable, but can be compensated for. This is the case of attenuation and Compton scattering in the patient, Compton scattering in the detectors, partial volume effects, variable spatial resolution across the field-of-view. In PET, accidental coincidences might also be a source of inaccuracy. Truncation artefacts due to limited-angle geometries, or ring artefacts also hinder quantification. Motivated by the advance of novel technologies such as TOF-PET or PET/MR, novel methods able to compensate for attenuation by simultaneously estimating the activity distribution and the attenuation have been proposed.

One main source of image degradation is patient and organ motion. In particular, cardiac and respiratory motion (in thorax or abdominal examinations), and involuntary head motion in brain studies might strongly distort the information content of the images. Several strategies to deal with motion have been proposed (see reviews in Rahmim *et al.*, 2007), which can be grouped into two categories: gating and non-gating methods. In gating methods, the acquired data are split in frames based on an external motion detection system. Assuming that there is little or no motion in the single frame, the frames are reconstructed individually with a standard algorithm. The external signal could be a respiratory belt for respiratory motion or an electrocardiography for a cardiac motion (or both, named "dual gating"). This simple method allows the motion effects on the image to be reduced, but at the cost of increased noise levels (i.e. worsening the signal-to-noise ratio). To overcome these limitations, much research is dedicated to the development of sophisticated non-gating methods, which do not rely on any external signal and, in general, make use of all the acquired data at the same time. The later approach leads to improving the signal-to-noise ratio, as shown in Figure 9. Among these approaches, there are strategies that assess separately motion and image, and other methods that jointly estimate motion and activity distribution (image). Regardless of the motion correction method, accurate quantification requires that the CT map and the PET images are acquired in the same respiratory conditions. In some cases, this is done by acquiring a 4D-CT that entails an increase of dose not justifiable for all the patients. To solve the dose burden of the 4D-CT, the group of Dimitris Visvikis proposed a method to generate dynamic CT images combining a reference CT image and the motion estimation of the 4D-PET.

3.2.2 Simulations

Monte-Carlo (MC) simulations have always been a fundamental tool in nuclear and particle physics, and have also become essential for the advancement of emission tomography [Harrison 2012]. MC simulations are often used to optimise the design of novel imaging systems or their components. Simulations are especially useful to examine the effect of a single physical phenomenon or a certain parameter, since the physics in real experiments is very complex and the effects of the underlying physical phenomena cannot be easily isolated.

Simulated data are also cardinal to test and optimise new techniques for data correction, image reconstruction, reconstruction of the interaction position within a detector, etc. Additionally, as mentioned in the former section, Monte-Carlo simulations are also used to calculate the system response model for image reconstruction.

Several multi-purpose packages for photon and particle tracking are being currently employed in emission tomography. Especially relevant ones are Geant4, EGS, MCNP, FLUKA, and Penelope. These packages can provide accurate simulations of the interaction of particles in matter, usually at the expense of large computing times, that might be prohibitive in the case of complex imaging devices. For these cases, dedicated simulation software, spe-

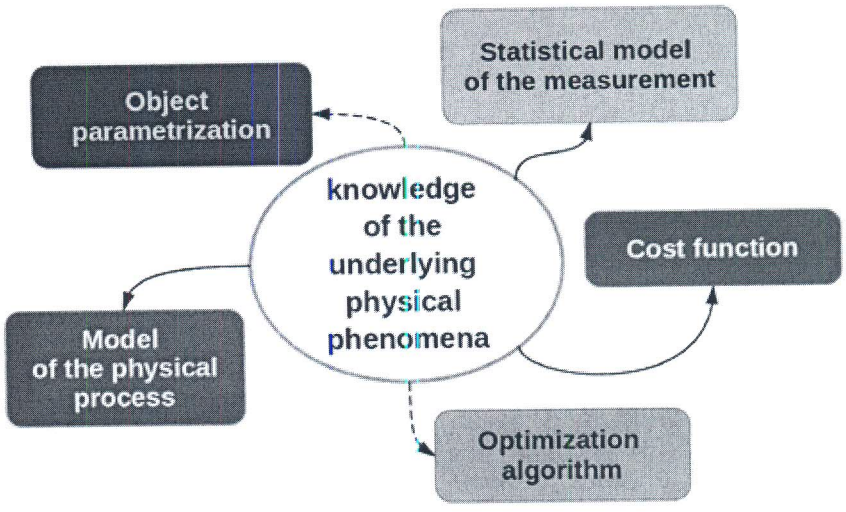

Figure 10. Sketch of statistical-iterative reconstructions. The information on the physical process, plus a statistical model of the measurement, is employed to estimate the data that should be measured in the scanner from a given parameterisation of the object. This estimate is compared to the actual data and a cost function, which may combine differences between estimates and data as well as regularisation criteria, is built and an optimisation function is called to minimise this cost function via modifications of the object.

cially conceived for photon-tracking in emission tomography, is usually preferred. Several packages have been developed for both PET and SPECT, such as GATE, SimSET, GRAY, or GAMOS, GATE and GAMOS being based on a GEANT4 framework. Some packages are PET specific (PETSIM, PET-EGS, PeneloPET, PET-SORTEO, or EIDOLON), whereas SiMIND was originally developed for SPECT. These dedicated packages are usually faster but less flexible than general-purpose ones. Simulating unconventional imaging devices might be difficult or even impossible without modifying the source code; however, for standard devices, they provide a number of interesting features such as detector electronics modelling, complex source and phantom description, or modeling of time-dependent phenomena.

As for image reconstruction, one main issue is to find a trade-off between accuracy and computing time. When speed is the main issue, analytical simulation packages, such as ASIM, might provide the desired performance. On the other hand, effort has been put in to accelerating simulations by parallelising the software or adapting it for distributed computing environments. A very promising alternative is the use of GPUs, which remains an active field of research.

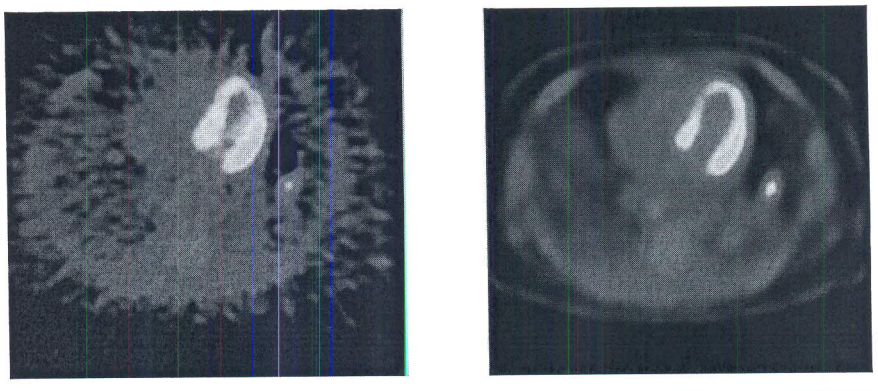

Figure 11. Reconstructed images from a clinical scanner. The data were reconstructed using analytical (left) and iterative (right) reconstruction algorithms.

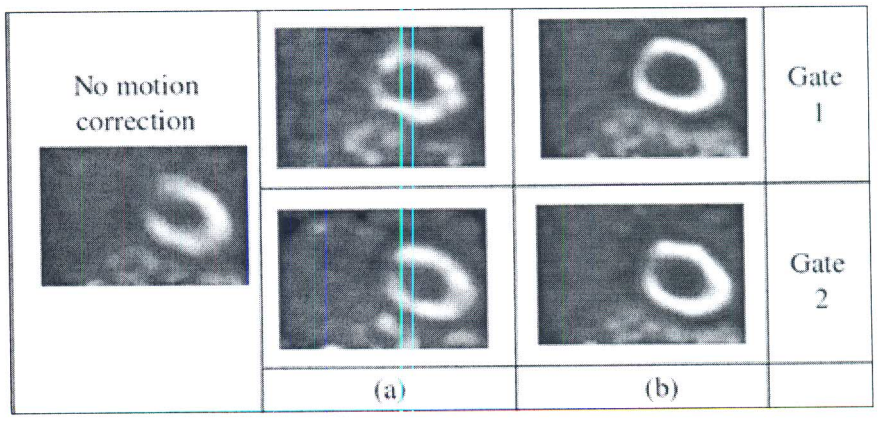

Figure 12. The effect of motion and its correction. Left column: no correction applied. Middle: A gate-based correction is applied. Right: Motion compensation is performed through simultaneous reconstruction of motion and image. The two rows correspond to different gates of very low statistics.

3.3 Photon counting: towards spectral CT

Hybrid pixel arrays applied to X-ray detection might provide a new generation of digital X-ray photon counting cameras that could replace conventional "charge integration" CMOS and CCD cameras used in X-ray computerised tomography (CT). Applied to the detection of X-rays, this technological breakthrough, which was originally developed for the construction of vertex detectors used in high energy physics experiments, can provide spectral information on the X-rays transmitted through an object. Thus, the current advent of X-ray photon counting cameras enables the development of spectral CT: a novel intrinsic anatomical and functional imaging modality that will hopefully open a new door in the field in molecular imaging.

3.3.1 Photon counting with hybrid pixels

Hybrid pixel detectors [Wermes 2005] form a new generation of digital X-ray cameras working in a photon counting mode that can replace conventional "charge integration" CMOS and CCD cameras used in X-ray computerised tomography (CT). This novel approach brings several advantages, such as the absence of dark noise, a high dynamic range and photon energy discrimination.

Hybrid pixel detectors have fulfilled these requirements quite successfully at the LHC at CERN and other nuclear physics experiments.

Hybrid pixels comprise the association of pixelised sensors and readout electronics connected through bump bonds (Figure 13). Usually, the sensor consists of n-type high resistivity silicon of a few hundreds nanometers thick with p^+ pixel implants, but it can also be from different materials of higher effective atomic numbers such as cadmium telluride

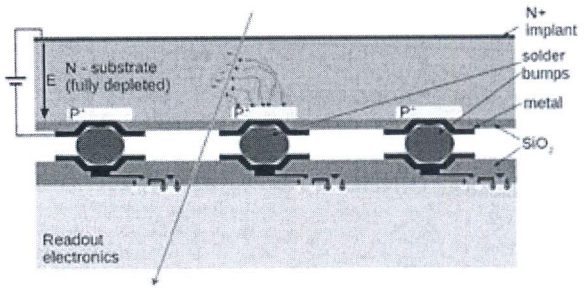

Figure 13. Schematic view of a hybrid pixel detector.

(CdTe), cadmium-zinc telluride (CZT) or gallium arsenide (GaAs), to provide better photon interaction efficiencies at X-ray energies up to 120 keV. The readout electronics chip (ASIC), which is pixelised at the same pitch as the sensor, is designed using standard CMOS processes.

The charges generated by photon interaction in the pixel sensor are collected on the ASIC via the bump bond connection and converted after an amplification stage in either a current or a voltage signal that is compared with one or several adjustable detection thresholds. Signals overcoming the threshold(s) are then stored in a local memory acting as a counter.

Several ASIC designs have already been developed, most of which so far have only one threshold, for the detection of X-rays using hybrid pixels (Table 3).

X-ray cameras consisting of an assembly of one or several modules of pixelised sensors bump bonded with hybrid pixel detector circuits have been built (see e.g. Figure 14) and have been used to pioneer spectral X-ray imaging.

3.3.2 Spectral X-ray imaging

In X-ray CT, the amount of X-ray absorption that induces a useful contrast for imaging depends on

Table 3. Technical specification of some hybrid pixel detector circuits.

	Number of pixels	Pixel size [μm²]	Count rate [counts/pixel/s]	Energy range [keV]	Threshold dispersion (r.m.s.) [e⁻]	Noise (r.m.s.) [e⁻]
Pilatus II	5'820 (60 × 97)	172 × 172	2×10^6	3 – 30	50	125
Eiger	65'536 (256 × 256)	75 × 75	16×10^6	4 – 30	20	180
Medipix2	65'536 (256 × 256)	55 × 55	10^6	5 – 30	360	140
Medipix3 (SPM)	65'536 (256 × 256)	55 × 55	10^6	6 – 30	55	72
XPAD3	9'600 (80 × 120)	130 × 130	10^6	5 – 60	57	130
PIXIRAD	243'712 (512 × 476)	60 hexagonal	10^6	1 – 100	–	50

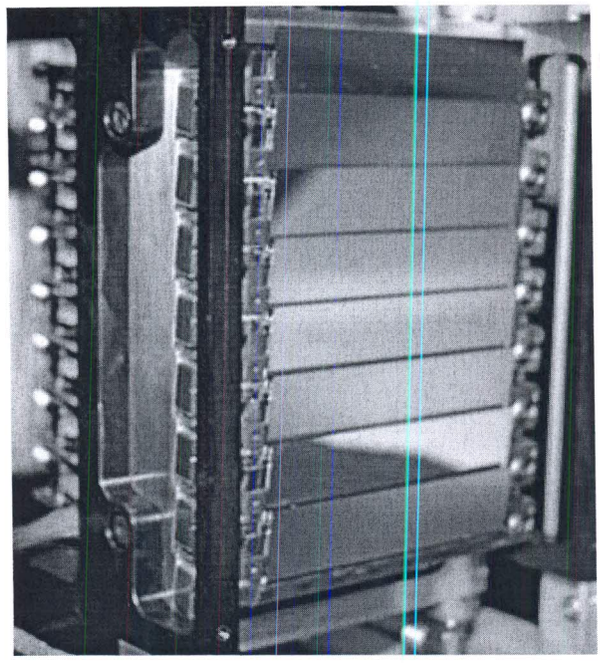

Figure 14. Picture of the XPAD3 camera composed of XPAD3-S ASIC, bump bonded to 500 µm thick silicon sensors to form horizontal modules. Eight modules of seven chips are tiled vertically to form a detector of 11 × 8 cm² composed of more than 500,000 pixels of 130 × 130 µm².

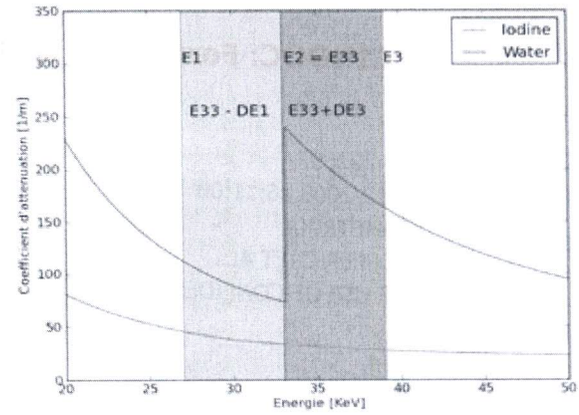

Figure 15. Principle of K-edge imaging of iodine (E_K = 33 keV).

the energy of the X-rays and the density and atomic composition of the matter they penetrate. In the past, several authors have pointed out the benefits of X-ray spectral information in computed tomography. Energy resolving detectors, with two or more energy bins, permit material decomposition thanks to the dependency of the attenuation coefficient on the X-ray energy, which is specific of each element. The increase of contrast-to-noise ratio for a given material can be maximised by choosing the optimal energy bins and/or by performing appropriate image weighting, either at the projection or at the reconstruction image level.

Moreover, when the energy of X-rays reaches the K-shell binding energy of the atoms that compose the traversed matter, the photoelectric absorption probability of X-rays increases sharply. This phenomenon is referred to as the K-edge. It is then possible to sense the atomic composition of matter by analysing these sudden absorption changes with energy. Subtractive analysis of X-ray absorption above and below the K-edge values of selected contrast agents such as yttrium (17 keV), silver (25.5 keV), iodine (33 keV), gadolinium (50 keV) or gold (80 keV) permit the identification of these contrast agents in a CT image.

Indeed, after energy calibration of the pixel, K-edge imaging can be obtained by changing the pixel threshold around the K-shell binding energy E_K of the selected contrast agent. In the case of detector pixels with only one energy threshold, images are acquired with three different thresholds: $E_1 = (E_K - DE_1)$, $E_2 = E_K$ and $E_3 = (E_K + DE_3)$ with DE_1 and DE_3 equivalent to a few keV. Thanks to the increase in absorption associated to its K-shell binding energy (Figure 15), subtraction of images reconstructed within energy windows $(E_2 - E_3)$ and $(E_1 - E_2)$ permit discrimination of the selected contrast agent. If more than two materials have to be quantified, more energy bins must be taken into consideration.

K-edge imaging has been demonstrated using small size (typically built using a single chip or a pair of chips) hybrid pixel detectors, as well as with the larger size XPAD3 camera (Figure 14) that permits scanning of a mouse without detector translation. As an example, Figure 16 shows the result of iodine and silver K-edge imaging of a phantom made of three twisted rubber pipes filled with silver, copper and iodine solutions.

Figure 17 presents maximum intensity projections (MIP) of standard absorption CT and K-edge scans of a mouse injected with 200 µL Iomeron®. A 50 kV, 600 µA X-ray spectrum was generated by a molybdenum anode tube filtered by 100 µm copper; 360 projections of 5 s were reconstructed with the FDK algorithm. K-edge imaging of the mouse suppressed bone structures that do not uptake iodine, while it reveals clearly the mouse kidneys and ureters.

3.3.3 **Prospects**

In a photon counting camera, every pixel can select X-ray photons above an energy threshold, or within energy windows when pixels have several thresholds, and count every photon individually without adding dark noise. Indeed, this feature cannot be achieved using conventional 'charge integration' CMOS detectors, because it necessitates settling quite a large amount of functions in a small surface that has to be smaller or equal to the pixel sensor surface. This makes a hybrid pixel detector ASIC

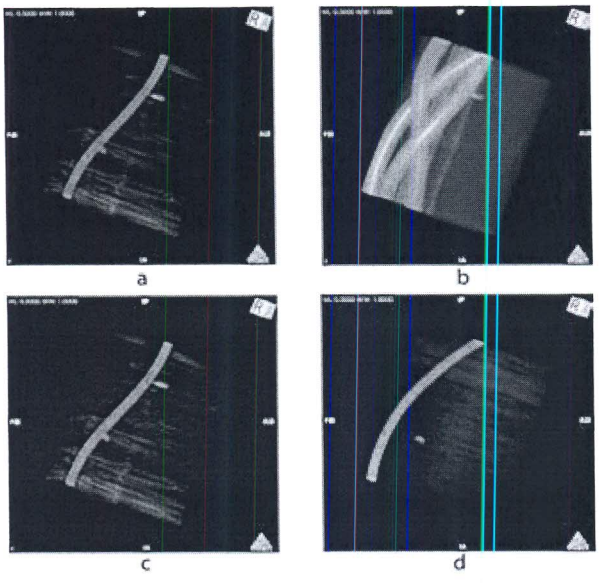

Figure 16. Transverse slice (a) and 3D volume rendering (b) of a phantom made of three twisted rubber pipes filled with Ag, Cu and I solutions. Data presented in (a) and (b) are acquired with a threshold of 25.5 keV and reconstructed using the FDK algorithm. 3D volume rendering of data obtained after subtractive analysis of X-ray absorption above and below the K-edge values of Ag (25.5 keV) and I (33 keV) are shown in (c) and (d), respectively.

quite a complex integrated circuit with several millions of transistor elements. Despite this difficulty, the technology of hybrid pixel detectors with silicon sensors is now rather well mastered and their performance correctly understood and modelled, which makes it possible to develop spectral CT for various applications.

As an example of a prospective application of spectral CT, let us consider glioblastomas, which are aggressive brain tumours with currently no treatment. Vascularisation and inflammation are two possible therapeutic targets whose relative contributions to tumour growth have to be characterised dynamically in vivo. Being able to image longitudinally both the tumour vascularisation and the inflammation would represent an invaluable tool to assess their effects on tumour growth. Markers of tumour vascularisation and inflammation can be labelled with gadolinium and iodine contrast agents used for magnetic resonance imaging (MRI) and CT, or gold nano-particles, which all have K-edges within the energy range of soft X-rays ($E_K = 33$, 50 and 80 keV for iodine, gadolinium and gold, respectively). K-edge imaging of gadolinium, gold and iodine is thus possible by processing subtractive analysis of X-ray absorption above and below their K-edges using X-ray photon counting detectors to select detected X-rays by their energies. As another example, it has been demonstrated that imaging of gold nano-particles can be used to study arterial inflammation and provide information on the composition of atherosclerotic plaque.

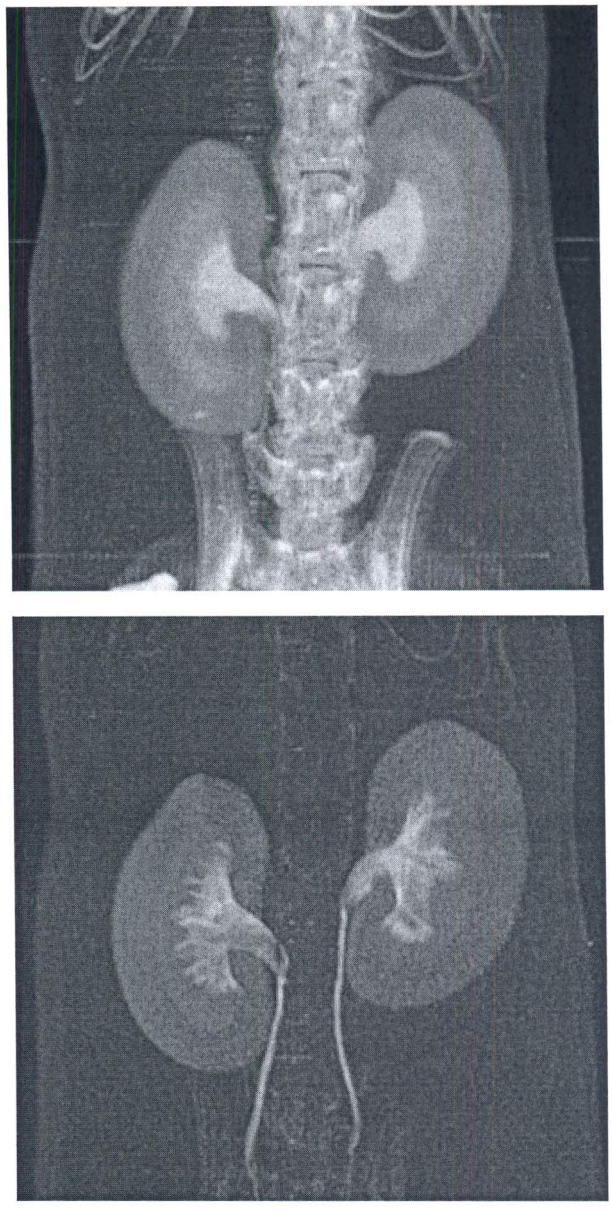

Figure 17. (top) MIP of standard absorption CT images. (bottom) MIP of K-edge images.

Nevertheless, X-ray absorption efficiency above 35 keV in silicon is only of a few percent, whereas more than 80% of X-rays interact in cadmium telluride above this energy. Thus the development of CdTe or GaAs hybrid pixel cameras is of utmost importance to address K-edge imaging above the iodine K-edge ($E_K = 33$ keV). At present, the relatively small diameters of CdTe or GaAs wafers do not permit hybridisation of large modules. Furthermore, CdTe wafers are quite brittle and can barely sustain mechanical stress, e.g. due to different dilatation coefficients of the CdTe sensor and the Si integrated circuit. However, given the energy range that is targeted by this new technology, the methodology developed on preclinical models, even using small size detectors, would be easily if not directly transferable to human clinics.

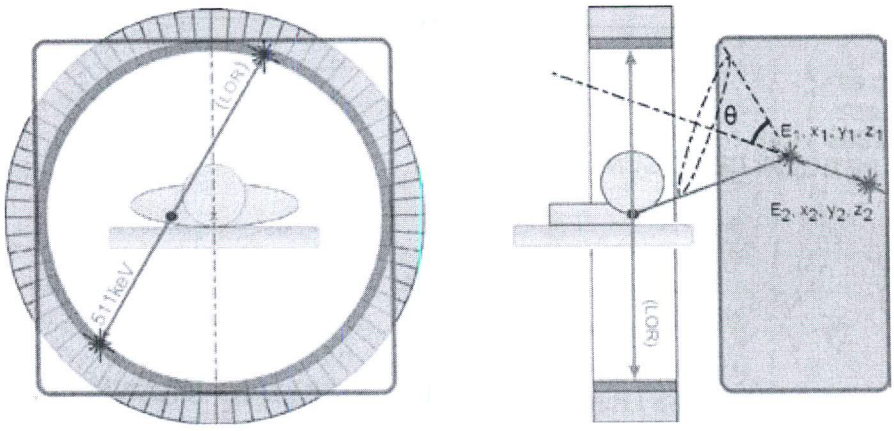

Figure 18. Schematic drawing of the '3γ imaging' principle based on the detection of a line-of-response (LOR) from two positron annihilation photons and a prompt third photon emitted from the excited PET isotope daughter nucleus. In this approach the additional photon is detected in a Compton camera formed by a cryogenic time-projection chamber filled with liquid xenon (from [Oger *et al.*, 2012]).

In summary, photon counting will potentially impact positively "black and white" or grey-scale CT accuracy by improving image contrast and signal-to-noise ratios. Indeed, with 'charge integration' X-ray cameras, the higher the energy of the detected X-ray, the more it will contribute to the formation of the detected signal, whereas with photon counting cameras, every detected photon contributes evenly to the Poisson statistics of the photon count. Hence, image contrast, which results predominantly from the detection of soft X-rays, tends to be better with photon counting CT than with charge integration CT. Furthermore, the rejection of low energy X-rays by photon counting detectors suppresses X-rays that are scattered with large angles and thus also tends to improve image signal-to-noise ratio.

More importantly, it is the ability of photon counting detectors to get spectral information on the detected X-rays that will bring a paradigm shift from "black and white" to "colour" CT. This will permit identification and/or discrimination of multiple contrast agents simultaneously, some of which will be nano-particles labelled with metallic elements identified from by their K-edge signature, and locate those within the anatomic grey-scale CT image, thus providing a large amount of functional information in vivo [Jorgensen *et al.*, 2011].

3.4 Nuclear medical imaging using $\beta^+\gamma$ coincidences: γ-PET

To date, a whole class of potential PET isotopes has been excluded from medical application. These are those where, in addition to the two back-to-back emitted 511 keV β^+ annihilation photons, a third higher-energy γ ray is emitted from an excited state in the daughter nucleus. The resulting extra dose delivered to the patient, as well as the expected increase of background from Compton scattering or even pair creation, has prevented the use of isotopes such as $^{44(m)}$Sc, ^{86}Y, ^{94}Tc, ^{94m}Tc, ^{52}Mn, or ^{34m}Cl. However, provided there is availability of customised gamma cameras, this apparent disadvantage could be turned into a promising benefit, offering a higher sensitivity for the reconstruction of the radioactivity distribution in PET examinations.

Presently two approaches are pursued towards the realisation of a medical imaging system based on β^+-γ coincidences. Both of them draw on the imaging properties of a Compton camera, where the registration of the Compton scatter and absorption kinematics of an incident photon in a suitable detection system (i.e. inelastic scattering of a photon with a (quasi-free) electron) is exploited to reconstruct the source position, within one event restricted to the surface of a cone (see Figures 18 and 19). Determining the intersection of this Compton cone with the line of response (LOR) as defined by the positron annihilation allows a sensitive reconstruction of the decay position of the PET isotope.

In 2004, a project was started in France, aimed at realising '3γ imaging' by combining a PET scanner with a Compton camera based on a cryogenic time projection chamber (TPC) filled with liquid xenon (LXe), acting simultaneously as scatter, absorption and scintillation medium for the additional 3rd photon. A small LXe-TPC prototype has yielded promising results [Oger *et al.*, 2012].

A second, more conventional, experimental approach pursued in several European laboratories utilises solid-state detectors to set up the Compton camera system. Here, double-sided silicon strip detectors serve as a Compton scattering unit, while scintillation crystals (either from well-established materials like BGO or LSO, or from novel scintillators like $LaBr_3$, see Figure 19) act as the photon energy absorber. Such modules could be combined with a ring of PET detectors (similar to the concept illustrated in Figure 18); alternatively a set of several Compton camera modules (as shown in Figure 19) could be arranged to detect either the

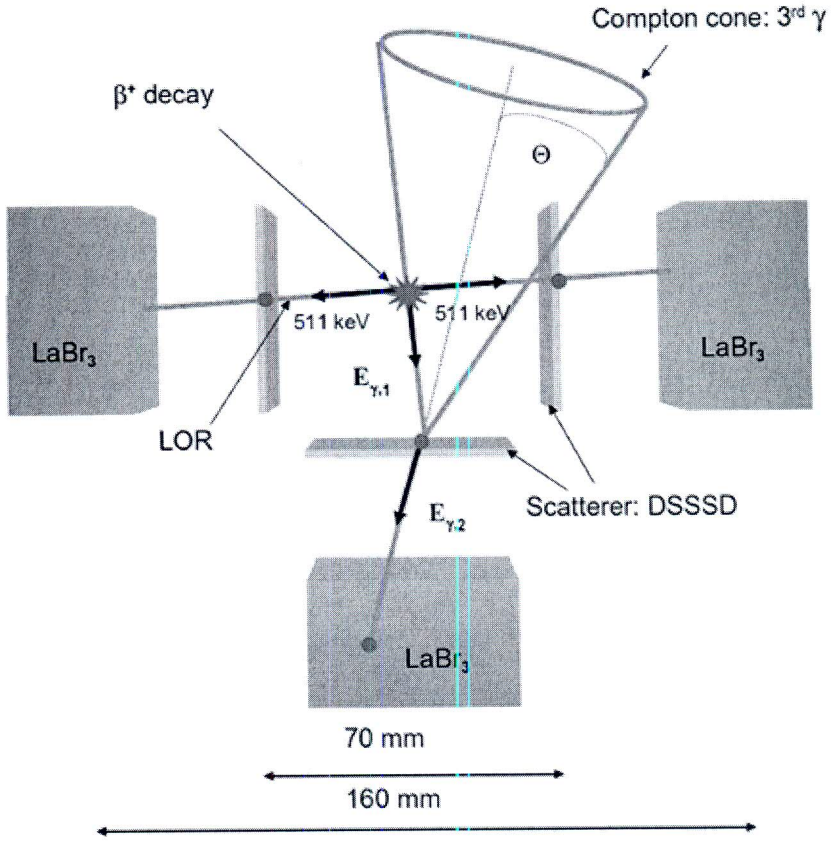

Figure 19. Arrangement of three Compton camera modules to define the LOR from β^+ annihilation in coincidence with the detection of the 3rd photon. Each module consists of a double-sided silicon strip detector (DSSSD) a scatterer and a $LaBr_3$ scintillator as absorber.

β^+ annihilation photons or the additional γ photon in coincidence.

The concept of $\beta^+\gamma$ coincidence imaging ('γ-PET') may open up the possibility to exploit a whole class of new PET isotopes, offering a highly sensitive and highly resolving localisation of the photon source position. The high sensitivity of γ-PET can be illustrated by the setup shown in Figure 19, where already a few tens of reconstructed intersections between the LOR and the direction towards the 3rd photon are sufficient to localise the activity contained in a voxel size of 2x2x2 mm^3 [Lang *et al.*, 2014]. In order to achieve the same with a conventional PET-based analysis, a few thousand LORs would be needed to be reconstructed. Beyond Europe, the topic of 'unconventional' PET isotopes is studied, for example in the US; however, so far no dedicated project to develop a 'γ-PET' detection system has been reported.

Finally, this technique would also provide the opportunity for building a 'hybrid detector', where during hadrontherapy treatment prompt photons could be detected from nuclear reactions of the therapeutic proton or ion beam with the tissue, while in the treatment delayed emission of photons from $\beta^+(+\gamma)$ decay of online produced β^+ emitters ($^{10,11}C$, $^{14,15}O$) could be detected.

4. Interfaces

4.1 Quality control in hadrontherapy

The main physical advantage of charged hadrons (i.e. protons or light ions) in radiation therapy is based on their finite range in tissue, with no or only a minor exit dose after a Bragg peak (see Chapter 1, Hadrontherapy) placed at a given depth depending on the energy at the entrance and the interactions in the path of the beam. However, in clinical practice significant uncertainties remain and the exact position of the beam range is not known with the required precision. Main factors contributing to range uncertainties in the order of several millimetres are summarised in Table 4, in addition to possible slow or fast anatomical changes in the body during or in between fractions. Methods for reducing range uncertainties can be classified in different categories and as a function of the time they are put in operation (Table 5). While pre-treatment dosimetric quality controls and cross calculations are most commonly used in current clinical practice, in vivo verification methods would represent an optimal solution for full exploitation of the advantages afforded by the ion beam.

Table 4. Uncertainty in range [Paganetti 2012].

Source of range uncertainty in the patient	Range uncertainty
Independent of dose calculation:	
Measurement uncertainty in water for commissioning	± 0.3 mm
Compensator design	± 0.2 mm
Beam reproducibility	± 0.2 mm
Patient set up	± 0.7 mm
Dose calculation:	
Biology (always positive)	+ 0.8%
CT imaging and calibration	± 0.5%
CT conversion to tissue (excluding I-values)	± 0.5%
CT grid size	± 0.3%
Mean excitation energies (I-values) in tissue	± 1.5%
Range degradation; complex inhomogeneities	- 0.7%
Range degradation; local lateral inhomogeneities*	± 2.5%
Total (excluding *)	**2.7% + 1.2 mm**
Total	**4.6% + 1.2 mm**

To date several methods of medical imaging in ion beam therapy are being investigated, including within the framework of a dedicated European effort (European NoVel Imaging Systems for ION therapy, http://envision.web.cern.ch/ENVISION/), in order to measure the range of particles in tissue or even directly measure the applied dose in vivo. Positron emission tomography (PET) is currently the only clinically applied method for in vivo range verification during or shortly after irradiation, and its potential benefit for ion tumour therapy has been proven. Further treatment verification methods based on the detection of secondary nuclear reaction products are prompt gamma imaging and charged particle imaging, which are currently under investigation. Another promising imaging tool in particle therapy is ion radiography and tomography, which is intended to be primarily used for position verification and treatment planning, but also can serve as a range verification method. In the following, all of these imaging techniques are presented. They require deep knowledge on nuclear processes as well as substantial abilities in detector design. Apart from challenging reconstruction tasks, the development of such imaging techniques also requires the simulation of the expected distri-

Table 5. Methods for beam range verification.

Family of methods	Name	Method	Short description	accur [mm]	Comm
Virtual	Calculation	Cross calculations	Use of different image data (e.g. dual energy CT) and models (e.g. Monte Carlo vs analytical)	2 - 4	estimation of uncertainty
Physical	Pre-treatment off line	Dosimetry	Dosimetric characterisation with different dosimetric systems	1	measurement in homogeneous media
	Pre or during treatment, upstream	Integrated electronic range verifier	Measurement around the border of the beam, arranged at different water equivalent depths // "transparent" detector (not existing yet)	2	upstream measurements in beam border
	Online in vivo verification	Prompt secondary imaging	Detection of prompt secondaries (prompt gamma, charged particles, neutrons?) emitted during treatment	?	in vivo, nuclear interactions
	Online-offline in vivo verification	PET detection	Detection of tissue activation (C, O,...) by nuclear interactions of the beam using PET imaging in the treatment room or close to it	1-3	in vivo, nuclear interactions
	"1D range probe", "2D radiography" and "3D ion CT"	Measure residual range or energy	Measure of residual range after traversing the body to validate the integrated stopping power and/or to reconstruct images of stopping power ration perform/validate calculations with finite ranges	1	feedback to calculations
	Implanted detector in path or tumour	Measure time pattern from an implanted detector	For modulated passive beams, the time signal of a detector synchronised with the modulator can be used to calculate the residual range	2	need implant
	Implanted detector after the target	Measure signal on the distal range or with higher energy	Implant a detector just after the target (e.g. in a rectum balloon, in a dental mold), measure a low dose at the fall off, or use a higher energy for a short irradiation	1	need implant in critical area or additional dose
Anatomy	Imaging post treatment	Magnetic resonance imaging	Visualisation of variations in images of irradiated tissue	2- 3	post treatment

butions. Therefore, extensive modeling of nuclear and electromagnetic interactions is necessary.

4.1.1 Positron emission tomography in particle therapy

Particles impinging on tissue induce, among others, positron emitters due to nuclear reactions with the atoms of the irradiated tissue. These positron emitters undergo radioactive decay according to their respective half-life, and positrons are released. These positrons annihilate with electrons of the tissue under emission of two annihilation photons with an energy of 511 keV each and an emission angle of approximately 180° (Figure 20). By means of a PET scanner, these annihilation photons can be detected in coincidence. Reconstruction of the measured events results in a 3D β^+-activity distribution.

The measured activity distribution cannot be compared directly to the applied dose distribution, since β^+-activity and dose originate from completely different physical processes.

Thus, a simulation of the expected β^+-activity distribution has to be performed on the basis of the treatment plan, under consideration of the time course of the irradiation and imaging. This calculated β^+-activity can be then compared with the measured distribution. The simulation has to model all physical processes from the electromagnetic slowing down and the nuclear interactions of the impinging ions and further secondary particles with the atoms of the tissue, the induction of

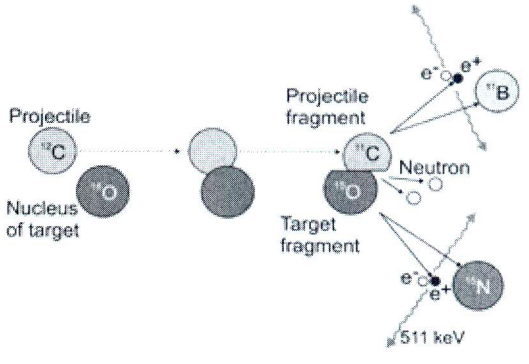

Figure 20. Principle of PET imaging in particle therapy for a ^{12}C ion (projectile) colliding with an ^{16}O atom of the irradiated tissue. Both nuclei may e.g. lose a neutron, resulting in the positron emitters ^{11}C and ^{15}O, respectively. They disintegrate under emission of a positron e^+, which annihilates with an electron e^- of the tissue. Annihilation photons with an energy of 511 keV each are emitted.

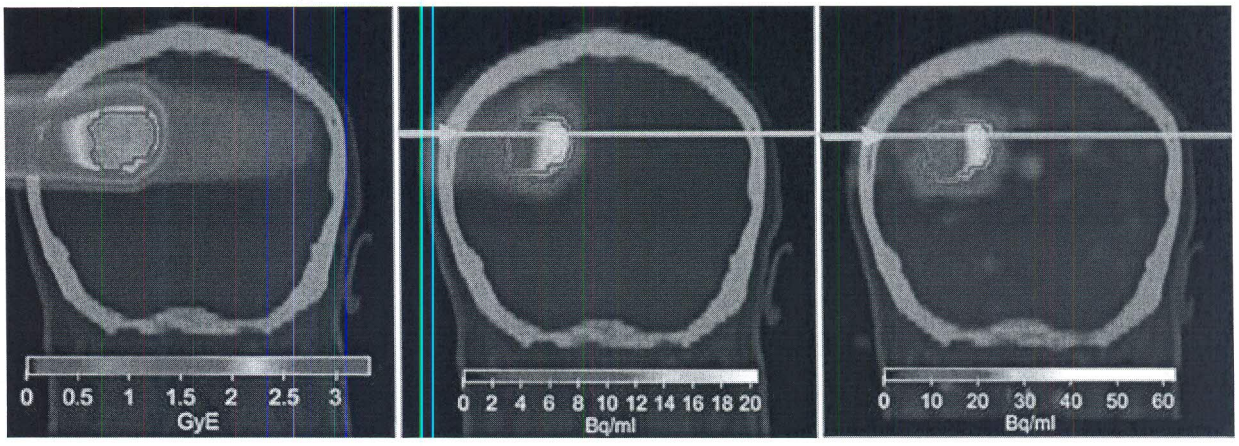

Figure 21. PET activation (right) measured after delivery of the planned carbon ion treatment dose (left) at HIT, in comparison to the corresponding PET MC prediction (middle). The arrow marks an example of good range agreement (adapted from [Bauer 2013] with permission).

positron emitters, the β^+ disintegration and formation of positrons, the thermalisation of positrons and annihilation with electrons, the transport and attenuation of the annihilation photons in the tissue until detection. All these processes require extensive knowledge of electromagnetic and nuclear processes, for example double differential reaction cross sections.

For PET imaging three implementations are investigated, which are described in detail in Shakirin 2011. The first is in-beam PET, which allows the measurement of β^+-activity during irradiation and requires a dedicated PET scanner integrated into the treatment site. The first in-beam PET scanner in clinical use was operated from 1997 to 2008 at GSI, Darmstadt, Germany. Another PET scanner directly integrated into the treatment gantry is located at NCCHE, Kashiwa, Japan, and is commercially available. Furthermore, small prototypes of in-beam PET scanners for research purposes are installed; for example, at HIMAC, Chiba, Japan.

The second modality is in-room PET. Here the PET scanner is located in the treatment room and imaging of the β^+-distribution takes place shortly after irradiation. An in-room PET scanner is investigated at MGH, Boston, USA.

The third modality is off-line PET, where no dedicated PET scanner is required, but conventional diagnostic devices, typically combined with CT scanners, can be used. After treatment the patient is transported to a PET system and the measurement of β^+ activity starts with time delays of several minutes, depending on the location of the scanner. This offline implementation is in clinical use, for example, at HIT, Heidelberg, Germany, and HIBMC, Tatsuno, Japan. An example of clinical application is shown in Figure 21.

Although already implemented in clinics, PET in particle therapy requires more technological and methodological developments. A major issue in future detector developments and a research field of several groups is the use of ultra-fast time of flight (TOF) information for PET monitoring in order to improve image quality. Further investigations are dealing with improvements on the knowledge of reaction cross sections, feasibility of PET for moving targets, application of PET for various other ions interesting for therapy, automatic evaluation of PET measurements, as well as application of PET in unconventional high energy photon therapy.

4.1.2 **Prompt gamma ray imaging**

During tumour irradiation with particles a large variety of prompt gamma emission occurs. These prompt gamma rays arise from nuclear de-excitation in an energy range of a few MeV. However, besides prompt gamma rays from the excited nuclei, in addition a substantial amount of background arises from other secondary particles, e.g. neutrons, light charged fragments as well as Compton scattered photons (Figure 22). Thus, several imaging modalities are being investigated to shield the background and selectively acquire information from prompt gamma emission.

A first approach is a collimated gamma camera, i.e. a collimator with a hole or a slit in front of a position-sensitive detector. A more advanced system is a multi-slit camera with a collimator with multiple slits in front of the detector. For those kinds of imaging systems, 3D information requires synchronisation with an upstream beam-positioning device such as a hodoscope.

Another possibility of prompt gamma ray imaging entirely independent from the treatment device is a Compton camera, which uses two or more energy- and position-sensitive detectors and, thus, no mechanical collimator is necessary.

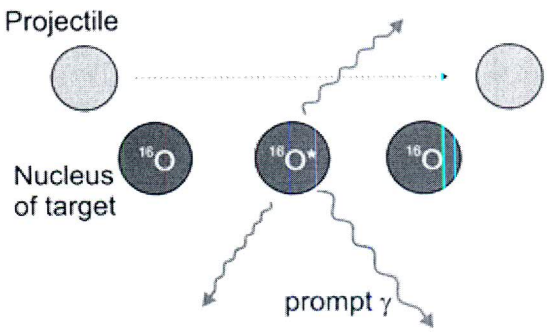

Figure 22. Principle of prompt gamma imaging using the example of a projectile ion colliding with an ^{16}O atom of the irradiated tissue. The target nucleus is excited and de-excites under emission of prompt gamma radiation.

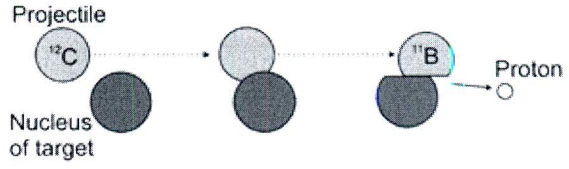

Figure 23. Principle of interaction vertex imaging shown for the collision of a ^{12}C ion with a target nucleus. The projectile ion loses a proton, which leaves the irradiated tissue and is used for imaging.

Improving detection efficiency and background rejection by means of a TOF gamma camera is also under investigation. It is supposed that discrimination between photons and hadrons becomes possible by using the time of flight information, although the time microstructure of the beam can be critical in this respect.

4.1.3 **Charged particle imaging**

During irradiation with primary ions heavier than protons, lighter projectile fragments are produced in collisions of the incident ions with nuclei of the irradiated tissue (Figure 23). Some of these light fragments have enough energy to leave the patient and can be easily detected. A reconstruction of the trajectory of the emerging charged particles and the intersection with the impinging ion path gives the point of ion– nucleus interaction. By means of a comparison between simulated and measured vertex distributions, the range of impinging ions can be verified. For this method, also known as interaction vertex imaging, a feasibility simulation study has been reported and the first promising measurements on homogeneous targets have been recently performed.

4.1.4 **Ion radiography and tomography**

Ion radiography enables the direct measurement of the residual range of high-energy low-intensity ions traversing the patient. It may replace X-ray radiography to produce low dose, high density resolution images of the patient at the place of treatment. In terms of pre-treatment verification, the method can be also used to validate in vivo the treatment planning range calibration curve deduced from the X-ray CT, which currently introduces the larger source of range uncertainties due to different physical processes of ion and photon interaction. Tomographic extension of radiographic imaging can enable volumetric images, providing a direct measurement of the ion stopping power ratio relative to water. Due to the weak energy dependence of the stopping power ratio, these images obtained at higher energies than for therapy can be used as a patient model in treatment planning, again eliminating the range uncertainties connected to the usage of calibrated X-ray CT images. Spatial resolution of the method is limited by multiple Coulomb scattering in the patient, which is more pronounced for protons than for heavier ions. However, 1 mm is anticipated to be achievable, even for the more scattering protons. New prototypes are currently under development both for protons and carbon ion beams.

4.2 **Mass spectrometry**

Mass spectrometry is a technique that was developed more than hundred years ago. It led to epochal discoveries, which laid the foundation to what is now called nuclear and particle physics. At that time it was a key method to explore atomic and subatomic particles, and in 1913 the seminal discovery of isotopes was made: that the chemical elements have constituents of different mass number. Since that time many more building blocks of matter were discovered and analysed in great detail, and besides its wide use and further development in nuclear physics, mass spectrometry found its application as an analytical tool in many fields of science, including chemistry, biology, geology, space science and many others[Mün13]. Besides these natural sciences, where analytical aspects dominate, there are a lot of applications, where mass spectrometry fulfills qualitative and quantitative requirements. These include environment, climate research, health, nutrition, security and many others. Here, we concentrate on health and medicine, with some emphasis on in situ applications. It is the goal of this section to introduce the reader to modern mass spectrometric techniques, sample preparation and present mass spectrometry applications for medical analyses and tissue imaging.

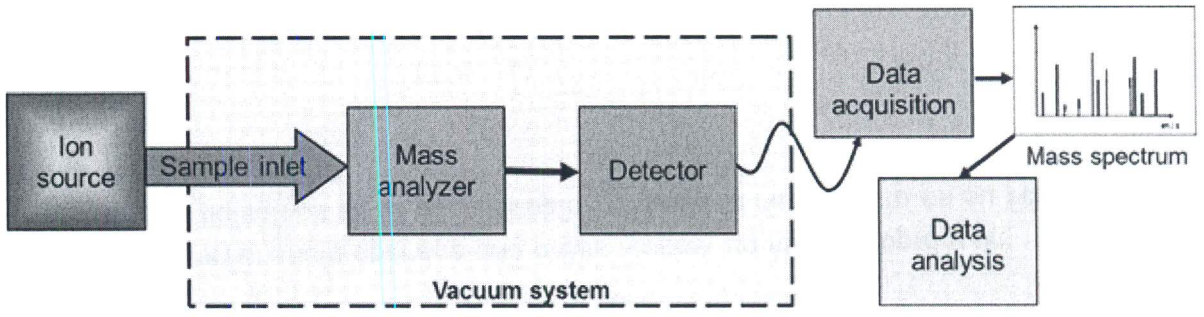

Figure 24. Schematic view of the components present in every mass spectrometer: ion source, mass analyser and detector. The vacuum system ensures that the ion motion does not suffer from collisions with gas atoms or molecules and is governed by the forces of electric and/or magnetic fields; this ensures that the spatial or time-wise separation of different species depends only on their mass-to-charge ratio.

Mass spectrometry

Mass spectrometry (MS) separates and analyses the building blocks and the chemical composition of a substance according to its mass-to-charge (m/z) ratio. Two principal concepts exist to disperse the ions: spatial separation and separation in time. The main elements, common to all mass spectrometers, are depicted in Figure 24: ion source (where the sample under investigation is transformed from its original form to ionised atoms, molecules or clusters), analyser (the central element, which disperses the ions timely or spatially according to their mass-to-charge ratio) and detectors (including data acquisition, storage, graphical display and quantitative analysis systems). Such devices all yield mass spectra, which represent the intensity distribution of the constituents of the sample, sorted according to an increasing mass-to-charge ratio. Today there are many types of ion-source and mass analyser, and a large variety of combinations of these exist, all specialised for certain applications. The most commonly used mass analysers comprise sector field magnets, quadrupole mass spectrometers, ion traps and time-of-flight (TOF) systems.

The performance of a mass spectrometer is characterised by several parameters. The most important ones being **mass range** (the range from the lightest to the heaviest mass that may be analysed, typically this ranges from one mass unit [hydrogen is the lightest chemical element] to a few 10,000 [which is typical for fragments of complex biomolecules like proteins]), **mass resolving power** (the ability to distinguish adjacent masses; this number should be high and ranges for routine operation from ~1,000 to 1,000,000), and **accuracy** (which is the ability to measure the true mass value of a certain species; inaccuracies should not exceed the ppm level). Besides these, other properties like the **sensitivity** of an instrument (the ability to investigate small amounts of sample material), the **dynamic range** (the ability to measure very rare and very abundant species simultaneously) or **scanning or non-scanning operation** (the former samples the mass range stepwise with the necessity of multiple scans to cover the whole mass range, while the latter covers the entire mass range at once) determine the potential for certain applications. Measurement duration as well as repetition rate are further critical properties for some applications.

Some modern instruments provide the capability of tandem-based analyses, the so-called MS/MS technique. With MS/MS sequencing, certain molecules can be selected in a first step, while in a second step the molecule is fragmented and the component pieces detected; by assembling the masses of each fragment, one can deduce the composition and obtain structural information; this works reliably for previously unknown analytes, especially when they are large and/or complex. The structure of complex biomolecules can be derived by this two-step analysis.

Present techniques for medical and imaging applications

Most specific for a certain application are sample preparation, ionisation and inlet techniques. Here, an almost infinite variety of concepts and techniques exist, tailored for the specific physical and chemical properties of the sample and the purpose of the analysis. The goal of all these techniques is to dissolve the sample by the impact of photons (e.g. laser light, which is used in laser ablation ion sources) or energetic particles (e.g. swift ions, which are used in secondary ion mass spectrometry, SIMS) or by desorption (e.g. by microscopic droplets of a solvent) such that it releases microscopic debris from its surface (atoms, ions and molecules), which can be analysed by the mass spectrometer. When such a focused ionising source is rastered in small steps laterally across a sample and for every pixel a mass spectrum is recorded, an "image" can be recorded

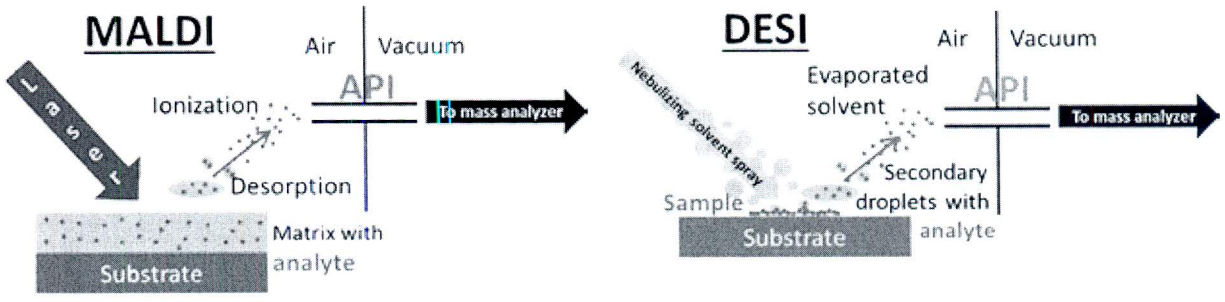

Figure 25. Desorption and ionisation techniques that are widely used in analytical mass spectrometry: matrix-assisted laser desorption ionisation (MALDI, left) and desorption electrospray ionisation (DESI, right). For details see text.

of how the constituents are distributed and structural information is obtained. Biological substances are often processed at ambient air pressure, while the mass spectrometer itself operates in a vacuum vessel; they are connected by an atmospheric pressure interface (API) and the sample fragments are introduced by various transport mechanisms that are simultaneously used to improve the selectivity towards the material of interest, but also to remove the necessity for pre-concentration of samples (enrichment) before analysis.

In imaging mass spectrometry (IMS), the original spatial composition and the integrity of the sample needs to be preserved, and analyte migration, degradation or contamination must be prevented to obtain original information. Figure 25 shows two concepts that are widely used in imaging mass spectrometry: matrix-assisted laser desorption ionisation (MALDI) and desorption electrospray ionisation (DESI). MALDI takes advantage of pulsed laser light impinging on an acidic matrix/solvent combination for extraction, desorption and ionisation of the substance from the surface, while DESI generates ions by a thin jet of electrostatically charged solvent, impinging obliquely on the sample surface. In both cases, the desorbed and charged sample debris are accelerated by an electric field towards the mass spectrometer and collected by its atmospheric pressure inlet system. Both techniques can be applied to basically any human or animal tissue.

Many other methods exist, which cannot be described here. They all have specific strengths and characteristic applicability to individual problems, depending on the sample, environment and purpose. Common to all is the generation of charged sample fragments that can be analysed by the mass analyser.

Present commercial IMS instruments reach a lateral resolution of the order of 10 to 50 micrometres (for comparison: the typical diameter of a mammalian cell is of the order of 5 to 20 micrometres), while research laboratories have reported sub-cellular resolutions down to ~1 micrometre. Typically, the ionising source rasters across the sample and the mass spectra yield characteristic information for each pixel, e.g. on proteins, peptides, lipids, etc. The overall area that can be sampled is in principle unlimited, but in practice depends on the speed of the instrument to record mass spectra and the overall available measurement time, so that typical areas of the order of a few square-millimetres or centimetres can be analysed. Large potential arises with three-dimensional imaging mass spectrometry, 3D-IMS. A stack of IMS images from the analysis of thin slices of three-dimensional objects can provide a detailed and comprehensive 'view' e.g. of an organ, including small tumour biopsies.

Medical applications of mass spectrometry and imaging

Imaging mass spectrometry, where high spatial resolution is combined with mass spectrometric analysis of the sample material, is a versatile and almost universal method to analyse the spatial distribution of analytes in tissue sections. An almost infinitely wide range of applications emerges due to the fact that basically every organic or inorganic material can be "dissolved" to microscopic fragments and ionised. The method is label-free and provides unique features for the analysis of tissues, especially when combined with classical histological stains. It provides specific information on proteins, peptides, lipids, drugs, neuropeptides and drug metabolites and many other biological substances. Since the measurements are performed on biological matrices, they require sensitive, high resolving mass spectrometers with high dynamic range able to handle the complex mass spectra. Medical benefits of MS range from new diagnostics, understanding of illness and its genesis to therapeutic developments. Examples are given in the following.

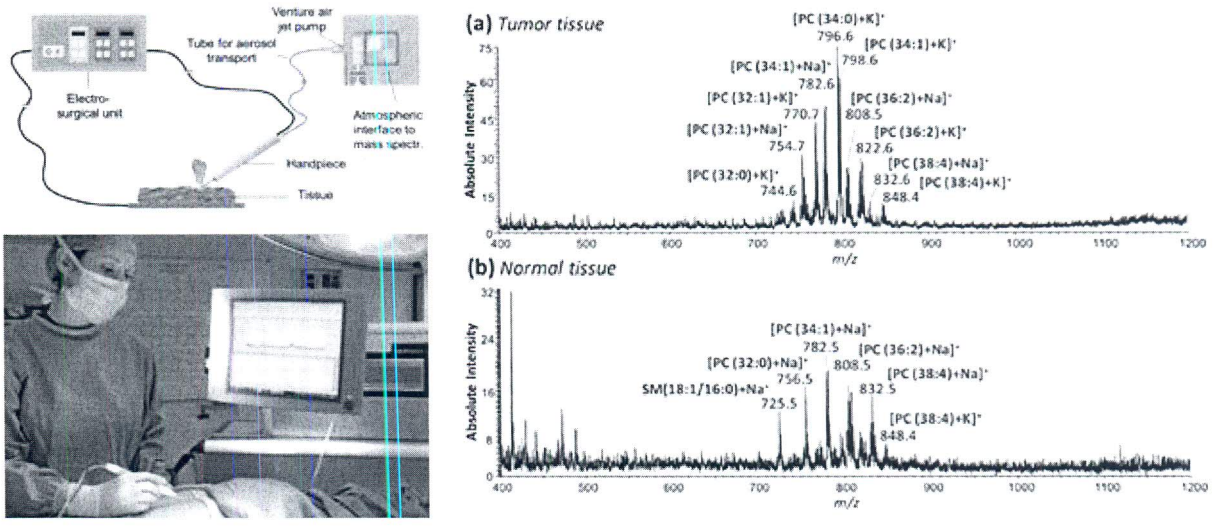

Figure 26. Top left: principle of an electro-scalpel in combination with an Venturi-pump inlet system for mass spectrometric analysis of vaporised tissue (reprinted with permission from Anal. Chem. 82, 7343. Copyright 2010 American Chemical Society). Bottom left: the device in operation during surgery (figure credit: Imperial College London). Right: mass spectra of a cancerous (top) and a healthy (bottom) human bladder tissue show different characteristic patterns (reproduced from *Faraday Discuss.* **149**, 247 by permission of The Royal Society of Chemistry, RSC).

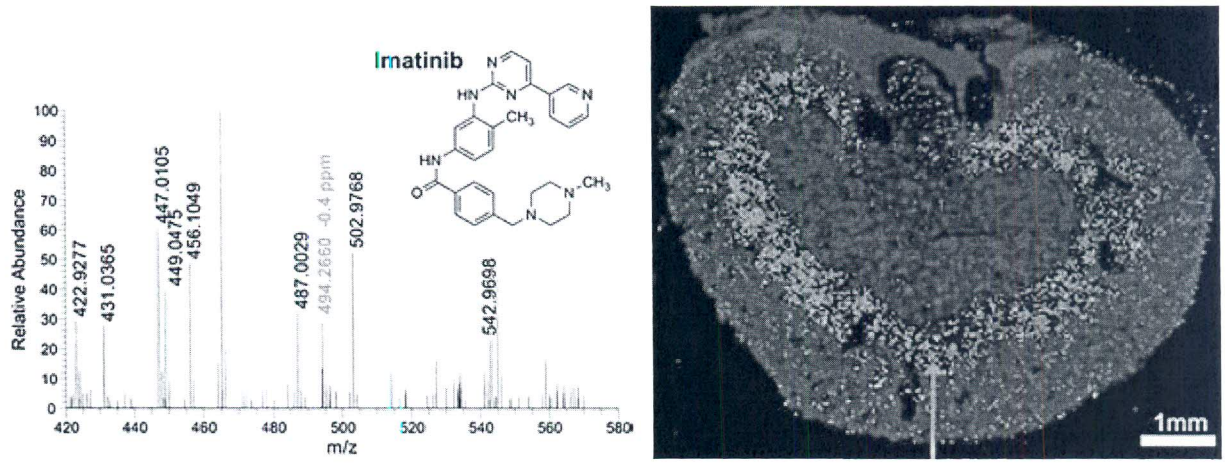

Figure 27. IMS spectra of a mouse kidney after treatment with the anti-cancer drug imatinib. Left: single-pixel mass spectrum of the outer stripe outer medulla; each pixel has an area of about 1/1000 square-millimetre. The green label indicates the mass peak that is characteristic for imatinib (m/z=494.2660). Right: imaging mass spectrometry yields the distribution of different substances in the mouse kidney. The green arrow points to the imatinib distribution, which is concentrated in the outer stripe outer medulla (figures reprinted from ref. [Röm13]).

• Tissue recognition

Very appealing is the potential of mass spectrometry for histology. Typical histological analyses take several hours. For intra-operative cases there exist faster (~30 minutes) but less reliable techniques. Here, fast and precise identification by means of mass spectrometry can be a solution. The tissue material is released by an electro-scalpel and transported into the mass spectrometer: heat is used to cut through the patient's tissue and produces tiny amounts of smoke that is rich in biological information. The "knife" collects some smoke, sucks it into the mass spectrometer and performs an instant mass spectrometric analysis. The obtained mass spectra exhibit different lipid profiles, which are analysed by multi-dimensional principal component analysis. Characteristic patterns indicate whether the cut tissue is cancerous or not. It also allows identification of metastases of various cancer types and to distinguish the original cancer from its metastases by different mass patterns. Figure 26 shows the principle of the electro-scalpel, its application in the operation room and examples of tumour and normal tissue.

• Multi-modal imaging

The above sections illustrate that IMS is a highly valuable method for studying biological samples. However, such samples are invariably complex and a single tissue section contains a large variety of chemical species ranging from salts, amino acids and lipids, to peptides and proteins. Therefore, the use of several different methods, each optimised for different types of molecules, enhances the infor-

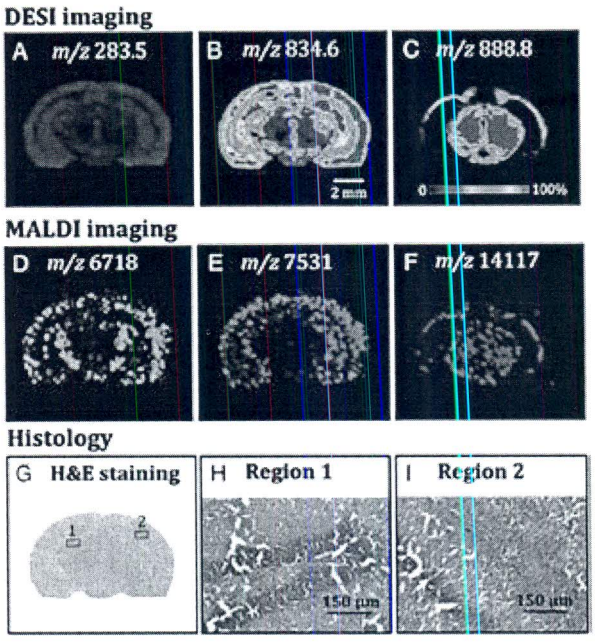

Figure 28. Complementary information on a mouse brain, obtained from different methods. The top and central row show intensity distributions of different lipid species imaged with a DESI source and of different proteins imaged with a MALDI source, respectively; the m/z values refer to various characteristic mass-to-charge ratios. Bottom: classical histological images using hematoxylin and eosin stain (H&E staining). Figure reprinted with permission from *Anal. Chem.* **83**, 8366. Copyright 2011 American Chemical Society.

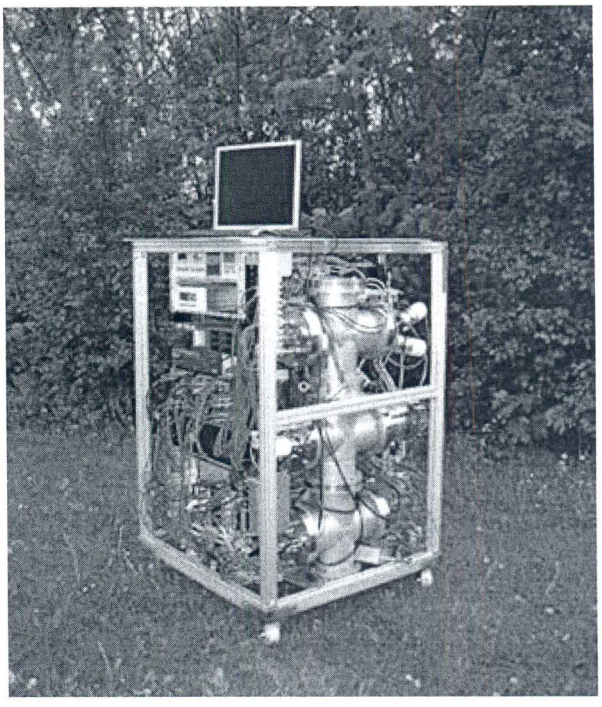

Figure 29. A modern example of a newly developed high-performance TOF mass spectrometer with ultra-high mass resolving power for in situ applications in environment, life-sciences and medicine.

mation gained by IMS. A good example is tissue samples of the brain, which are ideally suited for mass spectrometry analyses, since many of the relevant neuro-transmitters are either peptides or small molecules. Figure 28 shows an example of multi-modal imaging combining conventional H&E staining, DESI imaging mass spectrometry and MALDI imaging mass spectrometry. Each method was carried out on the same tissue slice of a mouse brain. The combination of information from each method provides a unique, complementary perspective by allowing analysis with each technique.

New developments for in situ applications with ultra-high mass resolving power

The growing number of applications and the analytical potential of mass spectrometry has stimulated the development of many different techniques, including miniaturised and portable apparatus for field deployment and use in many daily circumstances. A novel laboratory instrument for research and development is shown in Figure 29: this TOF mass spectrometer, originally developed for nuclear physics and astrophysical precision experiments, is compact, mobile, and it combines an atmospheric pressure interface for universal in situ analyses with ultra-high mass resolving power (in excess of 200,000). Envisaged applications in environment and life-sciences are, e.g.,

- *wastewater monitoring:* contamination of water with pharmaceuticals and personal care products are of increasing concern and represent a threat to wildlife and humans,
- *detection and identification of food contaminants:* there are numerous and steadily increasing numbers of contaminants, e.g. pesticides, natural toxins, veterinary drugs, food additives, adulterations or food-packaging migrants, that need to be identified and quantified, and
- *security:* the possibility of deployment of biological weapons by terrorists is an existing threat and effective detection and countermeasures are necessary.

The hitherto unrivalled combination of ultra-high mass resolution, MS/MS, non-scanning broad-band, IMS and in situ capabilities provides new analytical opportunities that will stimulate new field applications. These developments are a living example of how mass spectrometry methods and instruments, devised for nuclear physics experiments, continue to stimulate and cross-fertilise new applications in medicine and neighbouring fields.

5. Outlook

Medical imaging in general, and nuclear medicine in particular, for which detection of radiation emitted by the atomic nucleus is involved, has experienced and continues to exhibit evolution at exponential speeds. In the past, this evolution has largely benefited from technologies developed and tested in the experimental nuclear physics battleground, and it seems that this trend will only increase in the future. The maturity of the nuclear imaging sector can be seen by the fact that while in the past most nuclear detector technologies employed in the medical field, such as PMT and scintillators, were borrowed from the experimental nuclear physics knowledge base, nowadays new technologies are being pursued by the demanding medical industry, where the rate of technological evolution has never been so fast and new techniques are translated into biomedical research and clinical use within the year.

Nuclear physics groups have always been aware that their work in radiation detection, simulations, electronics, and data processing, might find application in nuclear medicine. But today we realise that our activities in these two fields are not only complementary and synergetic, but that their pace of development is very different. Nuclear physics experiments may take several years to design, fund, set up, run and analyse data. In the nuclear imaging arena, though, trends and technologies are being introduced, tested and dismissed at high speed. One can assess this by attending every year the leading conferences in the nuclear imaging instrumentation sector, such as the IEEE Medical Imaging Conference, and witnessing how the trends of previous year have been discarded and new ones are in the spotlight.

The urge to evolve nuclear imaging detectors is dynamising the activity of nuclear physics groups, while, on the other hand, mid-term stability in the scientific goals needed to face multi-national nuclear physics experiments, makes it possible to train and shape the best technicians, doctors, researchers and in general experts in technology for nuclear detection. There are many examples of researchers trained in nuclear physics groups doing basic research, who have later pursued successful careers in the medical imaging industry.

This chapter has provided a glimpse of how nuclear physics research has been involved in the advance of medical imaging and, more interestingly, how our current efforts are paving the way for the imaging technologies of tomorrow. X-ray spectral CT, PET/MRI scanners, devices for quality control of hadrontherapy, to name a few, will be commonplace in the most up-to-date clinical practice in a few years.

We have seen that multimodality in nuclear imaging has taken a big step forward in the last decade. This has mostly been driven by the introduction and widespread acceptance of PET/CT units in clinical practice, especially in oncology, and more recently by the deployment of simultaneous PET/MRI systems. In the preclinical field combined modalities are diffused and necessary, since the active groups are typically in academia where they can find the resources and knowledge to implement and develop the most highly sophisticated molecular imaging technologies available today. Just to address the hardware side, novel scintillators, photodetectors and DAQ systems have received a great boost from these activities, thus demonstrating the cross-fertilisation between the fundamental research in detector and technology carried out in nuclear physics groups and their application in molecular imaging.

We have also noticed that advances in instrumentation for medical imaging should be accompanied by corresponding advances in image reconstruction and modeling, in order to fully exploit the improved performance of novel devices and provide increased image quality. For this purpose, accurate models of the image formation and degradation processes should be developed for each scanner or prototype. These models should rely on a profound knowledge of the underlying physical phenomena and their interconnection. Increasing computing power and advances in computer technology should make feasible the implementation of these models as a part of image reconstruction, requiring the involvement of highly specialised experts, very often trained through participation in nuclear physics experiments.

This chapter reflects the fact that inside the nuclear physics community, research and development activities in medical imaging detector development coexist, at times even within the same research group. These developments prove that, even if from the outside it appears that basic nuclear physics activities are far from real world application, they in fact continue to provide the best field to test new technologies in detector, electronics and processing. Moreover, they help to obtain critical mass to interface with the medical imaging industry. We feel more than ever that it is our duty to help and promote the translation of developments from our nuclear physics laboratories and basic nuclear science experiments into practical tools for the clinical and preclinical environments.

References

[1] Bauer, J.; Unholtz, D.; Sommerer, F.; Kurz, C.; Haberer, T.; Herfarth, K.; Welzel, T.; Combs, S. E.; Debus, J. & Parodi, K. (2013). Implementation and initial clinical experience of offline PET/CT-based verification of scanned carbon ion treatment. *Radiother. Oncol.*, **107**(2):218–26.

[2] Defrise, M. & Gullberg, G. T. (2006). *Image reconstruction.*, *Phys Med Biol* **51**: R139–R154.

[3] Harrison, R. (2012). In: Grupen, C. & Buvat, I. (Ed.), *Simulation of Medical Imaging Systems: Emission and Transmission Tomography*, Springer Berlin Heidelberg.

[4] S.M. Jorgensen, D.R. Eaker and E.L. Ritman. (2011). "Biomedical spectral X-ray imaging; promises and challenges," in *Medical Applications of Radiation Detectors*, edited by H.B. Barber, H. Roehrig and D.J. Wagenaar, Proc. of SPIE, vol. **8143**, 814302.

[5] C. Lang *et al.* (2014). Sub-millimeter nuclear medical imaging with high sensitivity in positron emission tomography using $\beta^{+}\gamma$ coincidences, JINST 9 P01008. doi:10.1088/1748-0221/9/01/P01008.

[6] Massoud, T.F., Gambhir, S.S. (2003). Molecular imaging in living subjects: seeing fundamental biological processes in a new light. *Genes Dev.* **17**:545.

[7] T. Oger *et al.* (2012). A liquid xenon TPC for a medical imaging Compton telescope, *Nucl. Instr. Meth.* A **695**: 125.

[8] Paganetti H. (2012). Range uncertainties in proton therapy and the role of Monte Carlo simulations. *Phys. Med. Biol.* **57**:R99–R117

[9] Rahmim, A., Rousset, O., & Zaidi, H. (2007). Strategies for motion tracking and correction in PET. *PET Clinics*, **2**(2), 251–266.

[10] N. Wermes, "Pixel detectors for tracking and their spin-off in imaging applications," Nucl. Instrum. Meth. A541:150-165,2005

[Mün13] G. Münzenberg, Int. J. Mass Spec.349-350 (2013) 9-18: "Development of mass spectrometers from Thomson and Aston to present"

[Röm13] A. Römpp *et al.*, Histochem. Cell Biol. 139 (2013) 759–783: "Mass spectrometry imaging with high resolution in mass and space"

List of Contributors (Chapter II)

- **Faiçal Azaiez,** France
- **David Brasse,** France
- **Piergiorgio Cerello,** Italy
- **Christophe de La Taille,** France
- **Alberto Del Guerra,** Italy
- **Peter Dendooven,** Netherlands
- **Wolfgang Enghardt,** Germany
- **Fine Fiedler,** Germany
- **Ian Lazarus,** United Kingdom
- **Guillaume Montemont,** France
- **Christian Morel,** France
- **Alex Murphy,** United Kingdom
- **Josep F. Oliver,** Spain
- **Katia Parodi,** Germany
- **Marlen Priegnitz,** Germany
- **Magdalena Rafecas,** Spain
- **Christoph Scheidenberger,** Germany
- **Paola Solevi,** Spain
- **Peter G. Thirolf,** Germany
- **Irene Torres-Espallardo,** Spain
- **Jose Manuel Udias,** Spain